AD_____

Award Number: W81XWH-10-1-0769

TITLE: Site-directed nanotherapeutics to abrogate RRMS and promote remyelination repair

PRINCIPAL INVESTIGATOR: Damien D. Pearse, Ph.D.
Paul Dalton, Ph.D.

CONTRACTING ORGANIZATION: University of Miami
Miami, FL 33136-1002

REPORT DATE: March 2013

TYPE OF REPORT: Revised Final

PREPARED FOR: U.S. Army Medical Research and Materiel Command
Fort Detrick, Maryland 21702-5012

# REPORT DOCUMENTATION PAGE

*Form Approved*
*OMB No. 0704-0188*



| 1. REPORT DATE | 2. REPORT TYPE | 3. DATES COVERED |
|---|---|---|
| March 2013 | Revise Final | 1 September 2010 – 28 February 2013 |

**4. TITLE AND SUBTITLE**

Site-directed nanotherapeutics to abrogate RRMS and promote remyelination repair

**5a. CONTRACT NUMBER**

**5b. GRANT NUMBER**
W81XWH-10-1-0769

**5c. PROGRAM ELEMENT NUMBER**

**6. AUTHOR(S)**

Dr. Damien D. Pearse, Ph.D., Dr. Paul Dalton, Ph.D., Dr. Tim Dargaville, Ph.D., Dr. Mousumi Ghosh, Ph.D. and Dr. Tobias Führmann, Ph.D.

**E-Mail:** DPearse@med.miami.edu

**5d. PROJECT NUMBER**

**5e. TASK NUMBER**

**5f. WORK UNIT NUMBER**

**7. PERFORMING ORGANIZATION NAME(S) AND ADDRESS(ES)**

University of Miami
Miami, FL 33136-1002

**8. PERFORMING ORGANIZATION REPORT NUMBER**

**9. SPONSORING / MONITORING AGENCY NAME(S) AND ADDRESS(ES)**
U.S. Army Medical Research and Materiel Command
Fort Detrick, Maryland 21702-5012

**10. SPONSOR/MONITOR'S ACRONYM(S)**

**11. SPONSOR/MONITOR'S REPORT NUMBER(S)**

**12. DISTRIBUTION / AVAILABILITY STATEMENT**
Approved for Public Release; Distribution Unlimited

**13. SUPPLEMENTARY NOTES**

**14. ABSTRACT**
Multiple sclerosis (MS) is an inflammatory-mediated demyelinating disease of the human CNS. The clinical disease course is variable and starts with reversible episodes of neurological disability (remitting–relapsing (RR-MS) stage). This transforms into a disease of continuous and irreversible neurological decline. Phosphodiesterase (PDE) inhibitors can prevent injury-induced reductions of cyclic AMP as well as facilitate tissue protection, anatomical repair, and functional recovery. We hypothesized that PDE inhibitor containing nanoparticles (NP), surface modified with peptides that recognize proteins extravasated at sites of vascular disruption (clotting factors, ECM), would accumulate at regions of CNS demyelination, reducing tissue injury and promote remyelination repair at very low drug doses. Initial work for this award focused on the characterization of polymeric (poly(ethylene glycol-b-ε-caprolactone)) NP size, fluorescent dye or drug incorporation and their functionalization with surface peptides for site-directed targeting. It was demonstrated that peptides (i.e. NQEQVSP, DPEAAE and NIDPNAV) can be conjugated to the aminated PEG-b-PCL and that PEG-b-PCL NPs can readily encapsulate fluorescent dyes (DiI, DiO) and PDE inhibitors (Rolipram and BRL-50481). Whereas the loading efficiency of the fluorescent dyes was high (~45% and 80% respectively), drug loading was low in comparison, but could be improved by using more polymer. The drugs were released slowly over three weeks at 370C, after which the NPs started to aggregate/disassemble. Functionalization of the NP with peptides improved adherence in fibrin gels (blood clots) or onto tissue sections of injured spinal cord. In an experimental EAE model of RR-MS, we demonstrated that non-functionalized DiI NPs failed to accumulate at sites of EAE lesions following systemic administration, at a time just prior to the appearance of pathological changes and behavioral deficits. In contrast, the delivery of DiI laden, nidogen-1- or fibrinogen-functionalized NPs, showed that these NPs were sequestered to CNS lesions. Delivery of functionalized NPs encapsulating Rolipram, when delivered prior to disease onset, reduced the time of disease onset as well as decreased the severity of the disease score compared to non-targeted, Rolipram-laden NP controls. Histological evaluation of tissue samples revealed that the degree of demyelination within the lumbar cord as well as the numbers of infiltrating immune cells at perivascular lesion sites was reduced in animals receiving functionalized NPs encapsulating Rolipram.

**15. SUBJECT TERMS**
Nanoparticles, peptides, fibrin (blood) clot, factor XIIIa, nidogen, laminin, tenascin C, versican, multiple sclerosis, drug delivery, interferon-1a, phosphodiesterase inhibitor

| 16. SECURITY CLASSIFICATION OF: | | | 17. LIMITATION OF ABSTRACT | 18. NUMBER OF PAGES | 19a. NAME OF RESPONSIBLE PERSON |
|---|---|---|---|---|---|
| | | | | | USAMRMC |
| a. REPORT | b. ABSTRACT | c. THIS PAGE | | | 19b. TELEPHONE NUMBER *(include area code)* |
| U | U | U | UU | 28 | |

## Table of Contents

## INTRODUCTION

Multiple sclerosis (MS) is an inflammatory-mediated demyelinating disease of the human central nervous system. The disease usually strikes young adults and typically begins with neurological deficits, variable periods of remission and unpredictable but clinically reversible relapses. This remitting–relapsing RR-MS stage of the disease can persist for 10–15 years and is often followed by a course of continuously progressive neurological disability referred to as secondary progressive MS (SP-MS; Trapp et al., 1999; 2008). A hallmark pathophysiological response to CNS injury or disease is a dramatic reduction in levels of the ubiquitous second messenger, cyclic adenosine monophosphate, cyclic AMP (Pearse et al., 2004), a critical cellular component responsible for regulating vital intracellular functions that include cell metabolism, proliferation, survival and differentiation (Francis and Corbin, 1999). Levels of cyclic AMP in cells can be reduced by a family of enzymes called phosphodiesterases (PDE; Beavo, 1995; Souness et al., 1997). It has been shown that the use of PDE inhibitors prevents injury-induced reductions in cyclic AMP after acute CNS insults (Pearse et al., 2004; Atkins et al., 2007) as well as facilitates significant tissue protection, anatomical repair, and functional recovery (Pearse et al., 2004). However, despite such promise, dose-limiting side effects, primary of which are pronounced nausea and vomiting, have hampered their clinical development. Both the dose and multi-organ effects of PDE inhibitors could be reduced significantly, if the agent's release is restricted to the microenvironment of tissue pathology. To accomplish this goal, we sought to develop a delivery system in which PDE inhibitors, encapsulated within polymeric nanoparticles, would be specifically targeted to regions of vascular disruption through surface peptide sequences on the nanoparticles that recognize extracellular matrix (ECM) proteins or clotting factors which are extravasated on damaged blood vessels (Wallner et al., 1999; Kooi et al., 2009).

## BODY

The ensuing reportable outcomes and milestones combine data sets from both the Primary PI (Damien D. Pearse) and the Partnering PI (Paul Dalton) for the entirety of the award period. In line with the SOW, Study Objective responsibilities are allocated to each PI as indicated by surname (Pearse or Dalton). In accordance with the SOW, results and milestones are presented by Study Objective in numerical order with the associated tasks listed beneath. The final report provides data from the previous two annual reports as well as work performed during the NCE period, including the histological data piece for the performed studies (Task 10) as well as an update on manuscripts/abstracts associated with the work (Task 11).

### Study Objective 1: Prepare tNPs with surface-modified peptide incorporation [Dalton]

**Task 1 (Month 1-3):** *Synthesize peptides and obtain NP reagents*
**1.a.** *Synthesize ECM binding peptides*
The following peptides were synthesized:

| | |
|---|---|
| Fibrin – | **Factor XIIIa substrate** |
| Active: | NH2-CGGG**NQEQVSP**-COOH |
| Scrambled: | NH2-CGGG**VQENQPS**-COOH |
| | |
| Tenascin C – | **Versican** |
| Active: | NH2-CGGG**DPEAAE**-COOH |
| Scrambled: | NH2-CGGG**PAEDEA**-COOH |
| | |
| Nidogen-1 – | **Laminin** |
| Active: | NH2-CGGG**NIDPNAV**-COOH |
| Scrambled: | NH2-CGGG**IPANDNV**-COOH |

PEG-b-PCL (poly(ethylene glycol-block-ε-caprolactone)) was used as the amphilic blockpolymer (MW: 2000:2800, Mw/Mn: 1.15) to form the nanoparticles. N,N'-dimethylformamide (DMF) as the

solvent. Peptides were conjugated to α-amino-ω-hydroxy terminated poly(ethylene glycol-block-ε-caprolactone) blockpolymer (aminated PEG-b-PCL, MW: 5800:19000, Mw/Mn: 1.4) with succinimidyl 4-[N-maleimidomethyl]cyclohexane-1-carboxylate (SMCC). Fluorescencent dyes used were 1,1'-dioctadecyl-3,3,3',3'-tetramethylindocarbocyanine and 3,3'-dioctadecyloxacarbocyanine perchlorate (DiI, DiO respectively).

**1.b.** *Formulate Nanoparticles (NPs)*

The method to prepare nanoparticles was simplified. Whereas the polymer solution had to be added drop wise to stirring PBS in the original protocol, the developed protocol shortened this step to fast stirring of the two solutions. This resulted in a faster production of the nanoparticles. No difference in nanoparticle size between the different methods were observed.

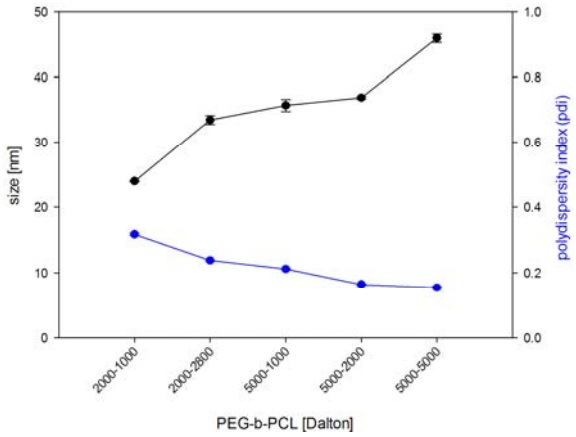


**Figure 1:** Size distribution and polydispersity index of PEG-b-PCL blockpolymers with different molecular weight.

Dynamic light scattering was used to identify the size of the nanoparticles. We tested different sized PEG-b-PCL blockpolymers with a molecular weight of 2 and 5 kDa of PEG and 1, 2, 2.8 and 5 kDa of PCL (**Fig. 1**). Increases in polymer size led to an increase in particle size, but a reduced polydispersity index. For further studies we choose PEG-b-PCL with a molecular weight of 2 and 2.8 kDa respectively, due to its favorable MW and nanoparticle size. A higher MW of PEG would increase the drug release (Shen-Guo and Bo, 1993) whereas the relative high amount of PCL can increase drug solubility (Letchford et al., 2008).

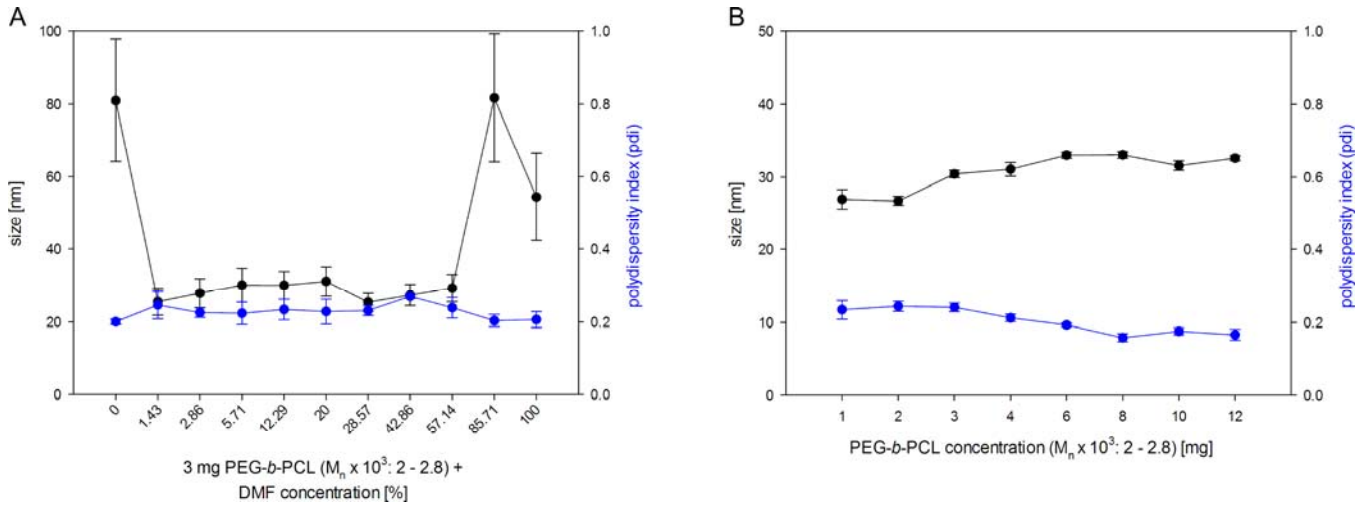


**Figure 2:** NP size and distribution is dependent on polymer and solvent concentration. **A:** Effect of DMF concentrations on nanoparticle size (n=3). **B:** Effect of polymer concentrations on nanoparticle size (n=3).

Low amounts of PEG-b-PCL (1-2 mg) led to a slightly smaller nanoparticle size than higher amounts (3-12 mg), where only slight variations could be found (mean range: 30-33 nm). Furthermore, using DMF concentrations ranging from 1.43 to 57.15%, resulted in similar sized NP (particle size range: 28 – 36 nm). The smallest nanoparticles were observed with 28.57% DMF, resulting in a nanoparticle size of 27.7+1.1 nm. In stark contrast, using only PBS (90+47.6 nm) or high concentrations of DMF resulted in a greater nanoparticle size and high variability (85.71%: 90+58.2 nm, 100%: 67.5+50). All NP demonstrated a low polydispersity index. Polymer concentration of 3 mg and DMF concentration of 28.57% were used for further studies (**Fig. 2A, B**).

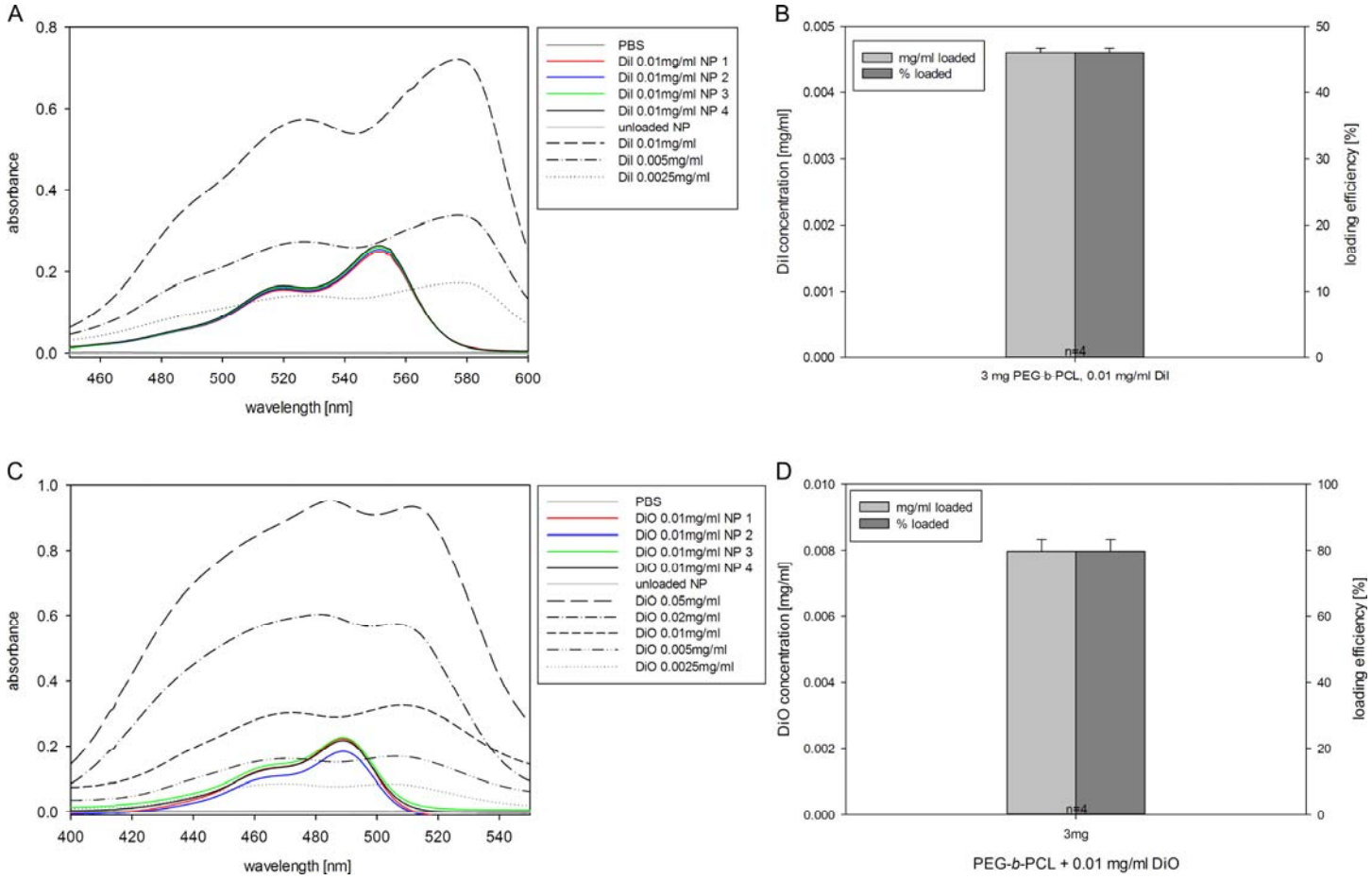


**<u>Figure 3:</u>** NP take up the fluorescent dyes DiI and DiO. **A, C:** Absorbance spectra for dye-laden NP, and free DiI and DiO at different concentrations. **B, D:** Loading efficiency and final concentration of DiI and DiO.

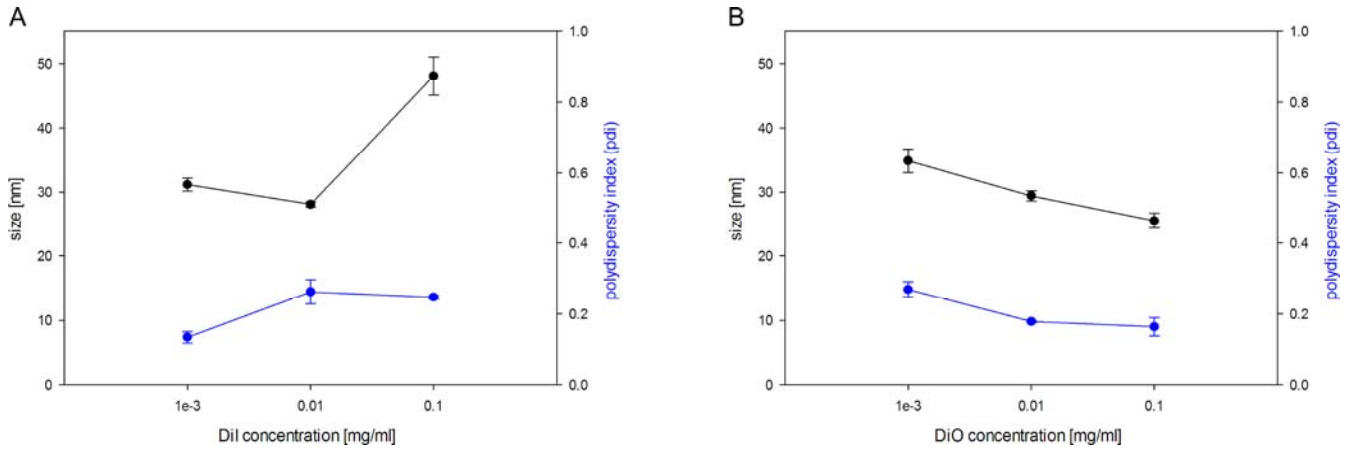

**Figure 4:** NP size and distribution was dependent on loading content (n=3). DiI (**A**) and DiO (**B**) NP demonstrated a low pdi with varying size, depending on loading content and concentration. Interestingly, higher concentrations of DiO led to a decrease in NP size.

Both fluorescent dyes were successfully incorporated into the nanoparticles when dissolved together with the polymer in DMF as demonstrated by measuring the absorbance spectra of the dye-laden NP (**Fig. 3A, C**). The dilution series of free dyes was used to calculate the amount taken up by the NP. The loading efficiency was good for DiI (~45%) and even higher for DiO (~80%, **Fig. 3B, D**). Interestingly, increased DiO concentrations led to a reduction in nanoparticle size (**Fig. 4B**). In contrast, higher concentrations of DiI led to an increase in mean nanoparticle size (**Fig. 4A**).

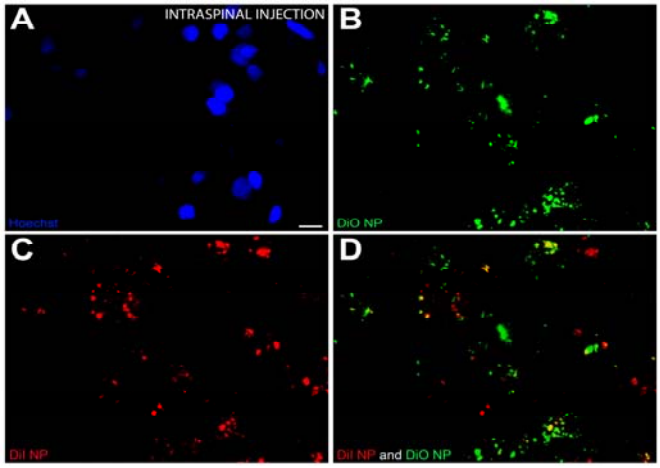


**Figure 5:** DiI and DiO loaded nanoparticles can be demonstrated in the injured spinal cord 24h after intraspinal injection (120 x magnifications). **A:** Hoechst (nuclear) counterstain (blue). **B:** DiO (green). **C:** DiI (red). **D:** overlay of B and C.

To test if fluorescent dye labeled nanoparticles can be detected *in vivo,* they were sent to Miami for injection into the injured spinal cord. At 24h after direct injection spinal cords were processed and observed with a confocal microscope. Both DiI and DiO labeled nanoparticles could be demonstrated within the spinal cord (**Fig. 5**).

**Task 2:** *Surface modify NPs with peptides*

**2.a. (Month 4-9)** *Incorporate different quantities of peptides into NPs and test binding efficiency*

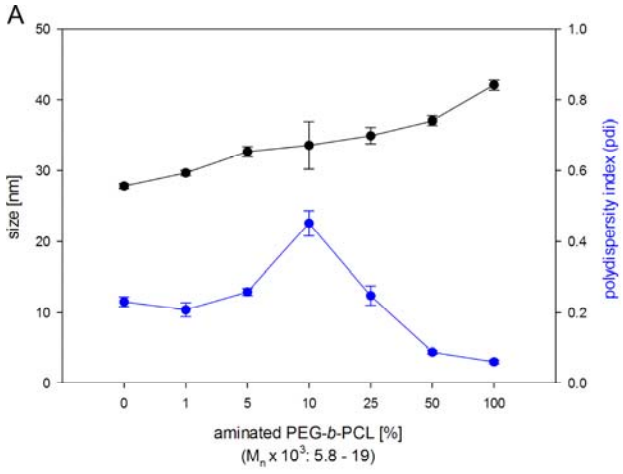


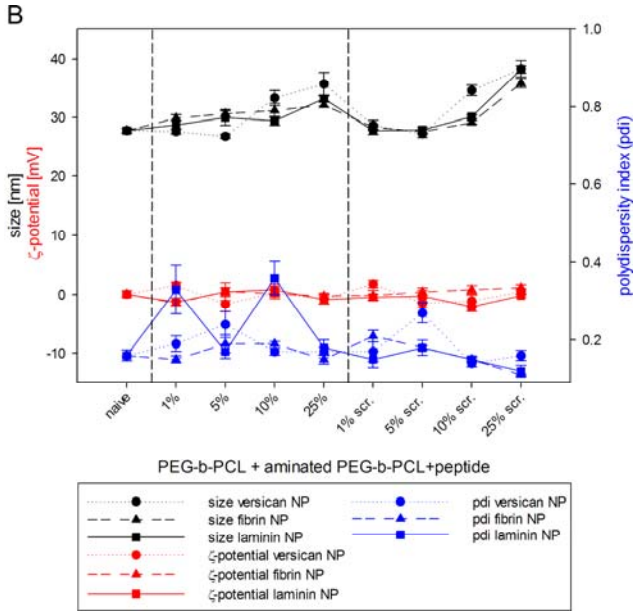

**Figure 6:** Functionalization of nanoparticles through inclusion of aminated PEG-b-PCL (**A**) and aminated PEG-b-PCL + different peptides (**B**) (n=3).

When the aminated PEG-b-PCL (1 to 100%) was mixed with the PEG-b-PCL containing solution before nanoparticle formation, the aminated PEG-b-PCL was successfully incorporated into the nanoparticles. Incorporation of aminated PEG-b-PCL led to an increase in nanoparticle size, with an increase in size when higher amounts of aminated PEG-b-PCL were used (Range: ~30-42 nm, **Fig. 6A**). The pdi initially increased, indicating a more heterogeneous size distribution of the nanoparticles, however using more than 10% aminated PEG-b-PCL led to a reduction again (**Fig. 6A**). Similar results were obtained with the peptide conjugated aminated PEG-b-PCL (Range: ~27-38 nm, **Fig. 6B**). Similar to the NP, functionalized NP demonstrated no surface charge (ζ-potential) and generally a low polydispersity index (**Fig. 6B**).

**2.b. (Month 4-12)** *Optimize binding and maximum peptide incorporation through NH2-PEG-PCL inclusion*

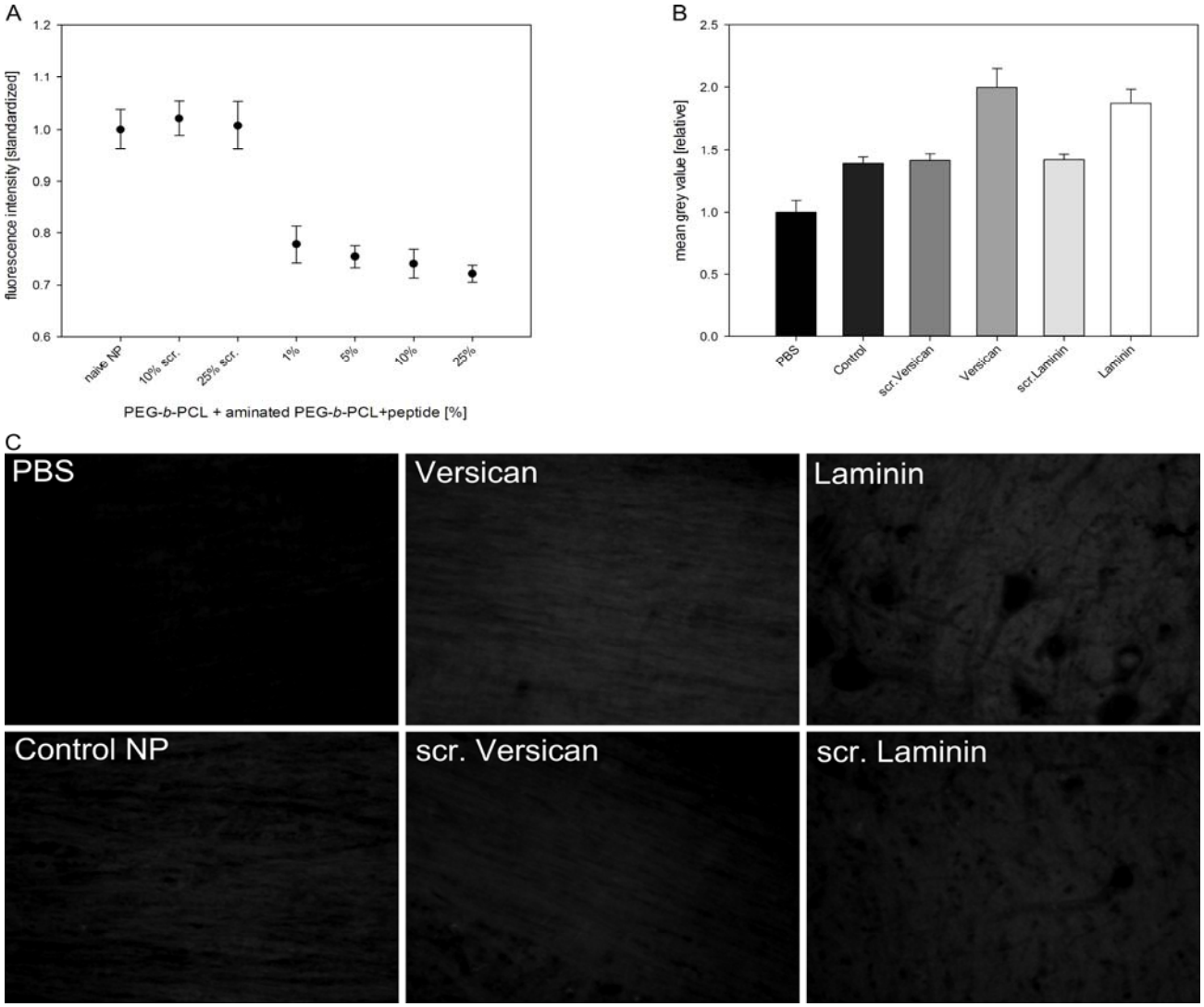


**Figure 7:** Peptide functionalization enhances NP binding. **A:** Nanoparticle release from fibrin gels *in vitro* demonstrates that fibrinogen functionalized nanoparticles bind better to fibrin gels than naive or scrambled peptide control nanoparticles (n=3). **B:** Nidogen-1 or Versican functionalized NP bind better to sections of the injured spinal cord (n=3). **C:** Fluorescence pictures of the NP bound to the spinal cord sections. Images were chosen after the average intensity value.

To test the binding capabilities of peptide functionalized NP in comparison to scrambled peptide and non-functionalized controls, NP were either embedded within fibrin gels (fibrinogen - NQEQVSP)

or incubated on sections of the injured spinal cord (nidogen-1, versican - NIDPNAV, DPEAAE). Scrambled peptide controls were used to see if the sequence itself has binding properties, even in a random order. NP binding to fibrin gels: The differences in the size of naive and peptide functionalized NP is minimal and should not lead to different binding properties in the fibrin gel. Peptide functionalization with the factor XIIIa substrate NQEQVSP (fibrin) lead to a greater retention of the nanoparticles in fibrin gels. The highest retention was reached with 10% and 25% (**Fig. 7A**). Since the best results for the fNP were obtained with 10% and 25% only those percentages of peptide incorporation were used for comparison to the scrambled peptide. The results show that the scrambled peptides are not retained within the fibrin gel and only reach values similar to the unmodified nanoparticles. Two more scrambled peptide sequences were investigated, with similar results (VENQPSQ and QVENQPS). NP binding to spinal cord sections: Spinal cord sections of contused spinal cords, one week after injury were used for this investigation. Peptide functionalized NP (25%, nidogen-1 and versican) demonstrated an increased binding ability to sections of the injured spinal cord compared to naive and scrambled peptide controls. Interestingly both showed unspecific binding and reached higher values than PBS (negative control, **Fig. 7B, C**).

**2.c. (Month 4-12)** *Determine the protein adsorption on the NPs by incubation with fluorescent proteins.*

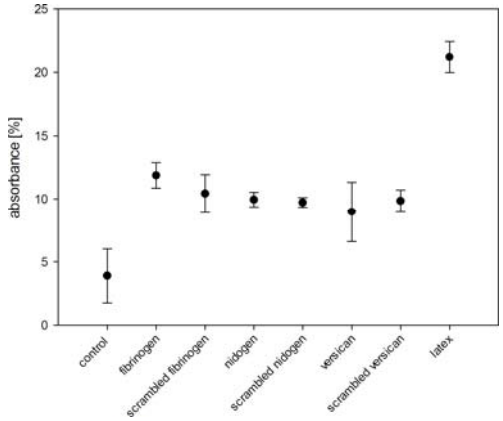


**Figure 8:** PEG chain prevents protein adsorption to NP. The different types of NP were incubated with bovine serum albumin (BSA) and the amount of NP that stuck to the BSA estimated by measuring the absorbance of the washed NP-BSA mix.

To determine the amount of protein adsorption on the different types of NP, they were incubated with BSA and the absorbance measured. Non-functionalized NP showed the least amount of protein adsorption (4%), due to the dense corona of PEG chains. Peptide functionalized NP were more prone to protein adsorption (9-12%), probably due to the peptide sequence (**Fig. 8**). However naive as well as peptide-functionalized NP had a lower ability to bind proteins on their surfaces when compared to latex beads (21%, positive control, measured by autofluorescence).

**2.d. (Month 4-12)** *Organize obtained chemistry data and discuss final formulations before proceeding*

Polymer concentration of 3 mg and DMF concentration of 28.57% were determined as the optimal formulation to investigate non-functionalized NP. Inclusion of 10% and 25% aminated PEG-b-PCL+peptide demonstrated the best results regarding fibrin targeting in vitro. Due to the lower pdi, 25% aminated PEG-b-PCL+peptide was chosen for further studies. Similar results were obtained for the other peptides (DPEAAE, NIDPNAV), which bound to sections of the injured spinal cord. To increase the nanoparticle concentration in solution, the amount of polymer was increased to 6 mg for in vivo delivery.

**2.e. (Month 4-12)** *Prepare significant quantities of the different types of tNPs for in vivo testing [Note: tasks 2a-d will be repeated for each peptide with sequential stock production to allow for in vivo testing to take place within 4 months of project initiation]*

Different types of NP (amount and type of peptide, controls, dye) were shipped to Miami for *in vivo* testing. Stock production did not seem suitable because long term storage of the NPs can affect their content and peptide properties. However NP can be stored for up to one month at 4°C, longer time points lead to decrease in drug content and reduced functionality of the peptides. Freezing of the NP without cryoprotection leads to disassembly; freezing with a cryoprotectant leads to aggregation and/or surface modification.

**Milestone 1: The production of characterized tNPs for each targeted protein**

Non-functionalized nanoparticles and fibrin, nidogen-1 and tenascin-c functionalized nanoparticles were completely characterized. No peptides against myelin are available at the moment, therefore targeting of this lipoprotein was not possible with our method.

**Study Objective 2: Screen tNPs for peptide modification that provides maximal NP targeting to EAE lesions [Pearse]**

**Task 3 (Month 1-3):** *Project organization and regulatory permissions*
**3.a.** *Submit and obtain animal approval*
**3.b.** *Plan and schedule studies*

Requests for animal approvals were submitted to U. Miami IACUC and ACURO and were received. Upon receiving the approval of animal experiments, planning for carrying out the studies under Objective 1 were scheduled with The Miami Project Animal Core Facility (housing for naïve and EAE animals, procedure rooms for inoculation). DVR staff members were also consulted about the timing of the study and the procedures reviewed.

**Task 4 (Month 4-9):** *Identify the temporal window of targeted protein production/presence after EAE*
**4.a.** *Purchase and acclimatize animals*
**4.b.** *Induce EAE in the animals*

Dark agouti (DA) rats were purchased from Charles River for acclimatization and EAE induction. The DA rats exhibited a very placid temperament and were easy to handle. To prepare the emulsion for EAE induction, spinal cords from 4 DA rats were extracted and prepared as homogenates, then supplemented with complete Freund's adjuvant and stored at -80 degrees for use in ensuing temporal EAE studies (Specific Aim 1B1). According to the experimental plan, animals were induced with EAE and survived for specific time periods thereafter for analysis of target protein by immunochemistry and immunoblotting.

**4.c.** *Perfuse animals and dissect tissues at different timepoints*
**4.d.** *Quantitatively measure protein production/presence by immunohistochemistry and immunoblot analysis*

Following induction of EAE, the behavior of the animals was recorded and their locomotor function scored daily according to the following criteria - 0: no disease; 0.5: distal limp tail; 1: limp tail; 2: mild paraparesis, ataxia; 3: moderate paraparesis, the rats trips from time to time; 3.5: one hind limb is paralyzed, the other moves; 4: complete hind limb paralysis; 5: complete hind limb paralysis and incontinence; 6: moribund, difficulty breathing, does not eat or drink, euthanize immediately. For the overall goal of these therapeutic studies, in which the NPs would first need to be given prior to the exhibition of pronounced functional deficits, we defined a behavior score range from 0.5 to 4.0 as being the optimal window for temporal analysis of target proteins. Based upon this behavior score range and the observed locomotor function of the animals after EAE induction, the temporal window of Specific Aim 1B1 was reduced to a maximum of 15 days (0 days, or the naïve control, and 5, 10 and 15 days post EAE induction; **Fig. 9**)

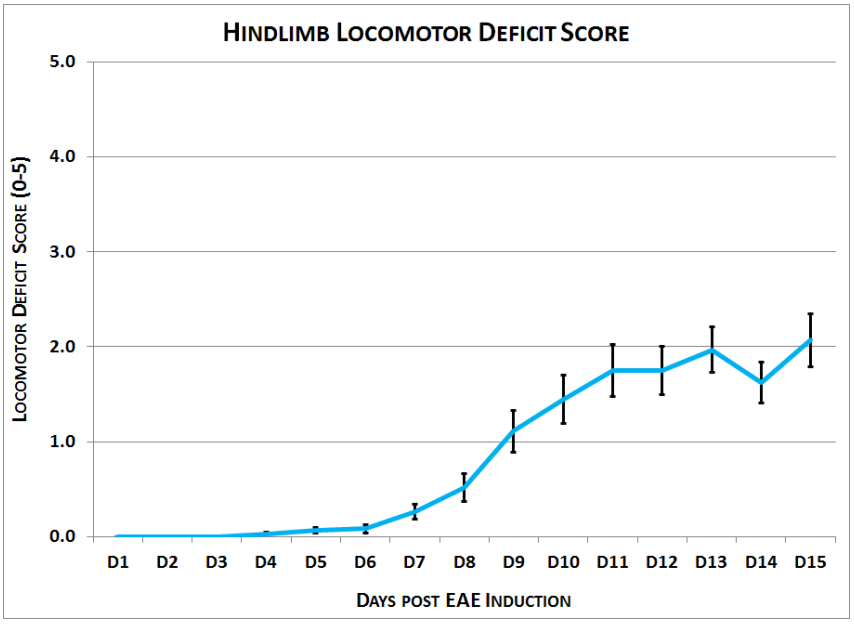


**Figure 9:** Temporal locomotor deficit scoring post EAE induction. Deficits were observed starting at ~7-8 days post EAE, pronounced hindlimb deficits (score =/>4) were observed in animals as early as 10 days post EAE (n=45 animals from D5, D10 and D15 cohorts).

Histopathological examination of the main target region of the CNS for EAE-induced blood-brain-barrier (BBB) permeability, immune cell infiltration inflammation and demyelination related to locomotor function loss, the lumbar spinal cord, using hematoxylin, eosin and luxol fast blue stained preparations revealed the presence of these pathological characteristics of EAE as early as 5 days post-induction in some animals (when behavioral deficits were first observed). By 10 days, and particularly by 15 days, post-induction these pathological features were observed to be present in all animals and were widespread and pronounced, correlating to a the greater degree of locomotor deficits (**Fig. 10**; see white arrows delineating pathology).

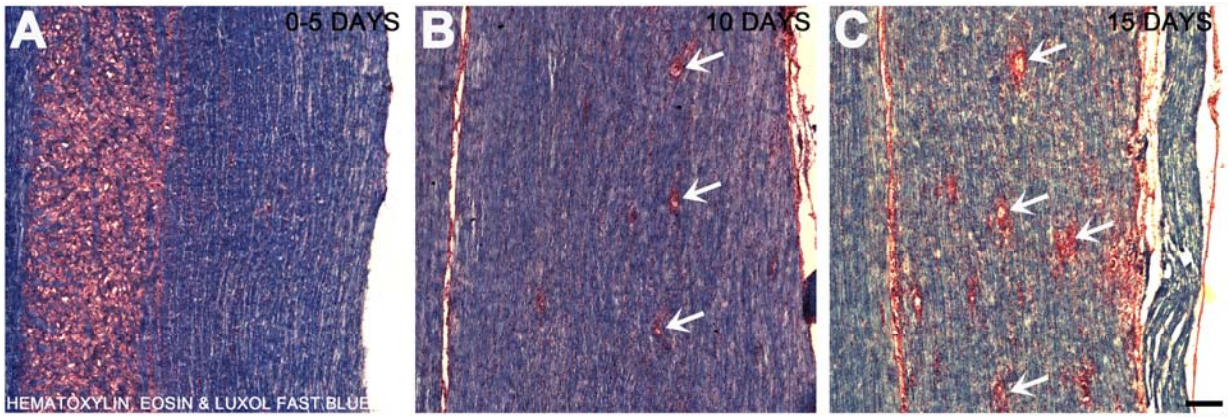


**Figure 10:** Histopathological characteristics of the chronic RRMS model of EAE. **A:** naïve spinal cord; **B:** 10 days post-EAE induction and; **C:** 15 days post-EAE induction.

Immunoblotting for target ECM proteins (fibrin and nidogen-1) and their natural ligands (Factor XIIIa and laminin) within lumbar cord homogenates from naïve animals and temporally post-EAE revealed a small increase in production of all proteins within 5 days of EAE over naïve levels, with all proteins exhibiting prominent and significant ($p<0.01$, 1-way ANOVA) increases by 15 days (**Fig. 11**; fibrin and nidogen-1 shown).

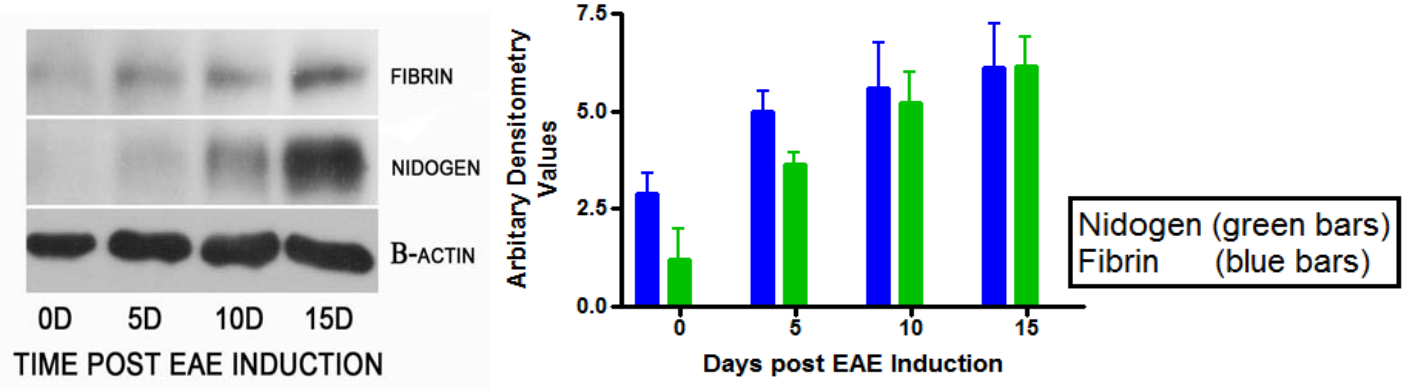


**Figure 11:** Temporal profile of target protein and natural ligand production post EAE as determined by immunoblotting.

Immunohistochemistry revealed that these proteins were highly concentrated within regions of BBB permeability, immune cell infiltration and tissue damage (**Fig. 12**; fibrin and nidogen-1 shown).

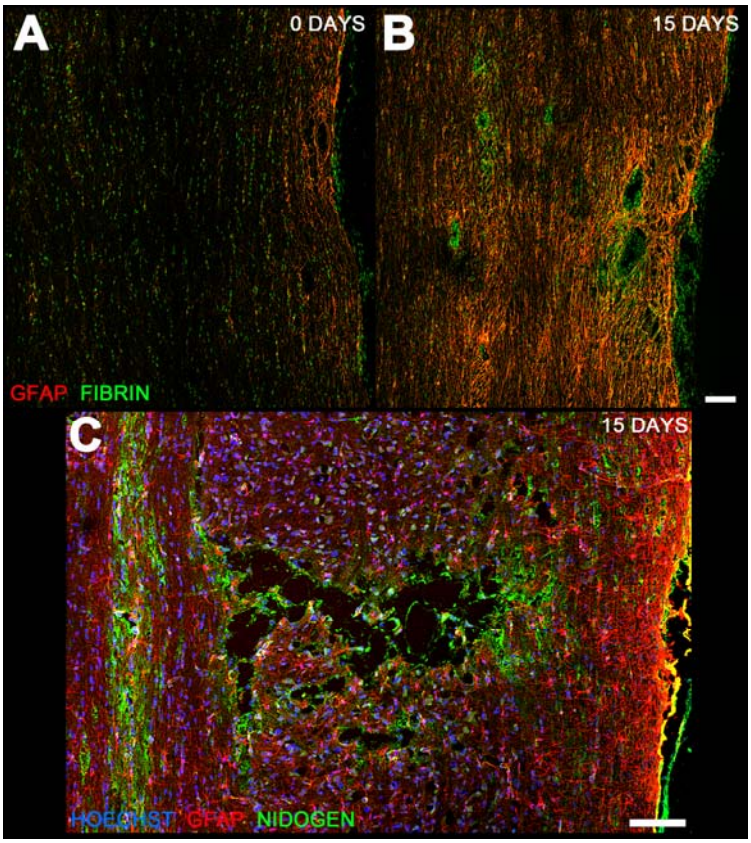


**Figure 12:** Immunohistochemical localization of target proteins and natural ligands within the lumbar spinal cord after EAE induction.

**Task 5 (Month 7-15):** *Test tNPs in an experimental MS model, EAE*
**5.a.** *Purchase and acclimatize animals*
**5.b.** *Induce EAE in the animals and provide fluorescent dye encapsulated tNPs (or unmodified NP controls)*
**5.c.** *Perfuse animals and dissect tissues*

Upon temporal characterization of target protein and their natural ligand production and localization after EAE, tNPs for fibrin and nidogen-1 (containing DiI and DiO), as well as non-targeted NP controls, were received from Brisbane for use *in vivo*. According to Specific Aim 1B2, DA rats were ordered and acclimatized. Based upon data obtained in the aforementioned tasks (temporal behavioral deficits, pathophysiology and increased protein production), tNPs and non-targeted

controls (labeled with DiI, 25% aminated) were initially administered intravenously beginning 10 days post EAE for 2 days. After 2 days the animals were perfused and sectioned for examination of NP localization within the lumbar spinal cord by confocal microscopy.

**5.d.** *Quantify the level of tNP accumulation at the site of the demyelination lesion*
**5.e.** *Identify those tNPs that did not exhibit target ligand binding following direct injection and re-formulate in vitro for re-testing in vivo*

Examination of lumbar spinal cords from EAE animals receiving non-targeted, DiI laden NPs failed to show fluorescent NPs within tissue sections. In the initial experiment using the first batches of NPs, only nidogen-1 tNPs containing DiI could be detected within the lumbar cord of EAE animals following i.v. infusion for 2 days, beginning during the initial spike of behavioral dysfunction (10 d post-EAE induction). Nidogen tNPs were found localized throughout regions of BBB permeability, immune cell infiltration and tissue damage after EAE and i.v. infusion (**Fig. 13**). Following the infusion of fibrin and versican tNPs containing DiI (first batch), no fluorescent signal was observed in the lumbar spinal cord of EAE animals.

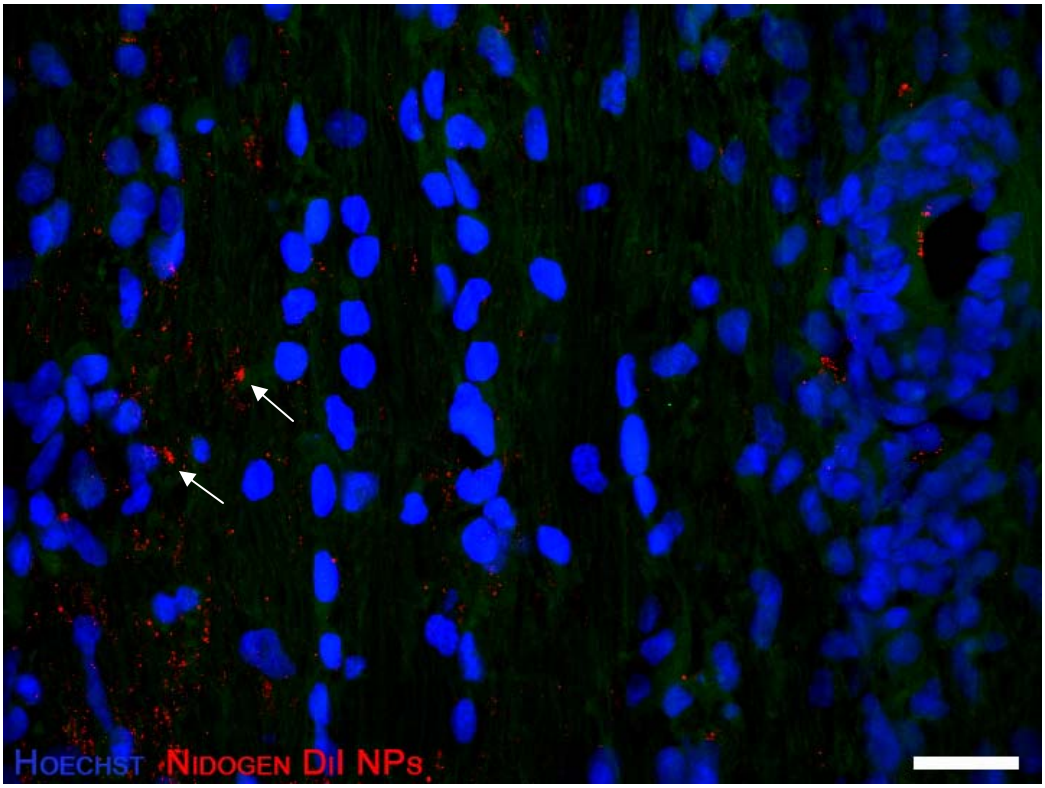


**Figure 13:** Localization of Nidogen-1 tNPs containing DiI within the lumbar spinal cord after EAE and tNP infusion for 2 days.

**5.f.** *Re-test any reformulated tNPs*

Upon completion of preliminary temporal testing of tNPs (Batch 1), reformulation and re-testing was performed to improve lumbar cord localization of fibrin and versican tNPs. In the reformulated tNPs (Batch 2), we identified a significant amount of fibrin tNPs, but only limited amount of versican tNPs, within the lumbar spinal cord of EAE animals following i.v. infusion (**Fig. 14**).

**Task 6 (Month 10-15):** *Organize obtained in vivo targeting data*
**6.a.** *Graph data and perform statistical analyses*
**6.b.** *Identify the optimal targeting peptide(s) for future testing of PDE delivery*
**6.c.** *Discuss ensuing studies, identify abstracts or manuscripts that can be prepared and patents that can be submitted*

We have confirmed our hypothesis that targeting of NPs to lesions of the lumbar spinal cord after EAE induction can be achieved when targeting peptides are upon their surface; this has been demonstrated using both nidogen-1 and fibrin tNPs. While the examination of lumbar spinal cords from EAE animals receiving non-targeted, DiI laden NPs failed to show fluorescent NPs within tissue sections, Nidogen-1 and Fibrin tNPs were found localized throughout regions of BBB permeability, immune cell infiltration and tissue damage after EAE and i.v. infusion (**Fig. 13, 14**). Unlike nidogen-1 and fibrin tNPs, versican tNPs were found only sparsely within the lumbar spinal cord of EAE animals following i.v. infusion (**Fig. 14**). The limited penetration of DiI-laden versican tNPs in spinal tissue could indicate that the levels of the substrate at 10 days post-EAE induction were too low, that the substrate was not present or extravasated at perilesional sites or that the targeting peptide had poor binding.

The discussion of abstracts and manuscripts from this work is presented at the end of the report under Task 11.

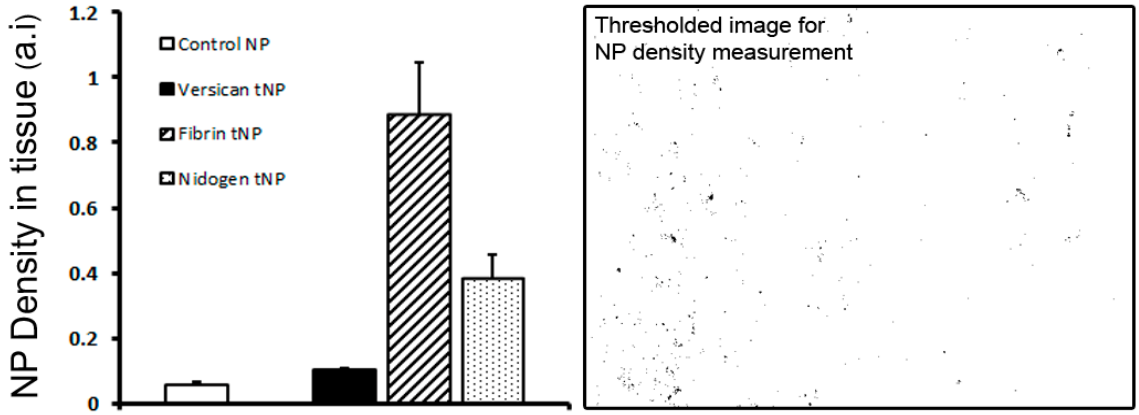


**Figure 14:** Measurement of DiI NP particle density in lumbar spinal cord tissue after EAE and infusion of different tNPs. Both fibrin and nidogen-1 peptide functionalized DiI-laden tNPs show significant accumulation in lumbar spinal cord tissue.

These results confirmed our hypothesis that targeting of NPs to lesions of the lumbar spinal cord after EAE induction can be achieved when targeting peptides are upon their surface.

**Milestone 2: Identified the optimal peptide(s) for targeting NPs to sites of CNS demyelination**

We confirmed our hypothesis that targeting of NPs to lesions of the lumbar spinal cord after EAE induction can be achieved when they are functionalized with peptides upon their surface (non-targeted NPs do not accumulate at these lesions); this was demonstrated using nidogen-1 and fibrin tNPs. Versican tNPs did not demonstrate good targeting capacity. This could be related to a low and disperse expression of the substrate after EAE, failure of the substrate to be expressed or extravasated at perilesional sites or to poor binding efficacy of the peptide. The ensuing efficacy studies using drug laden tNPs (Objectives 3 and 4) continued to employ all three tNPs to determine whether tNPs could provide anatomical and functional benefit in an experimental model of MS.

**<u>Study Objective 3: Prepare tNPs with the encapsulation of PDE inhibitors or interferon-1a [Dalton]</u>**

**Task 7:** *Synthesize peptides and obtain NP reagents*
**7.a. (Month 10-12)** *Synthesize ECM binding peptides*
**7.b. (Month 7-12)** *Formulate starPEG(sPEG) and PCL NPs*
**7.c. (Month 13-18)** *Surface modify NPs with optimal peptide(s)*

See Task 1.

**Task 8:** *Incorporation of PDE inhibitors or interferon-1a into tNPs*

**8.a. (Month 7-18)** *Incorporate different quantities of drugs and test release kinetics*

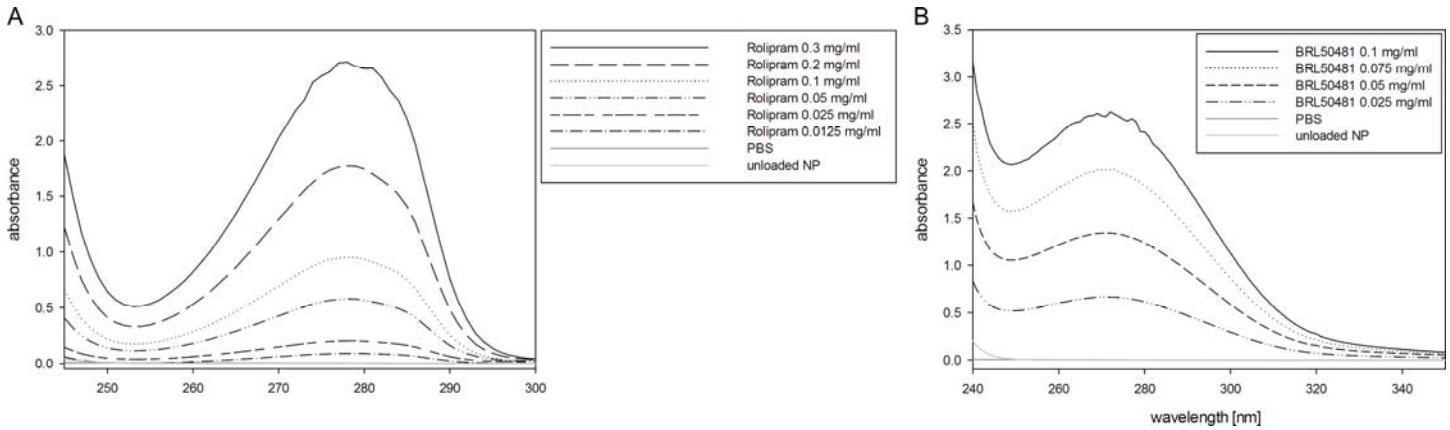


**Figure 15:** Absorbance spectra of Rolipram (**A**) and BRL50481 (**B**).

To measure the amount of drug taken up by the nanoparticles a dilution series of the two different PDE-inhibitors Rolipram and BRL50481 was performed and the absorbance spectra measured (**Fig. 15**). The drug content was calculated at a wavelength of 280nm.

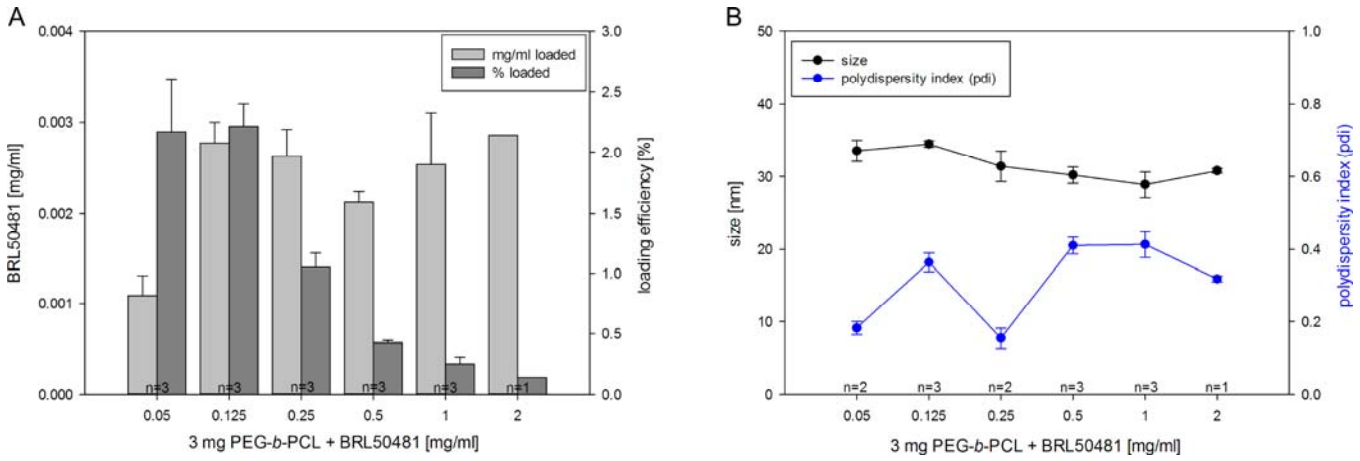


**Figure 16:** Loading efficiency decreases with increasing drug concentration. **A:** Drug loading content and efficiency of 3 mg polymer with different drug concentrations. **B:** NP size did not differ much with different drug concentrations, however the pdi varied, with no clear indication of a concentration effect.

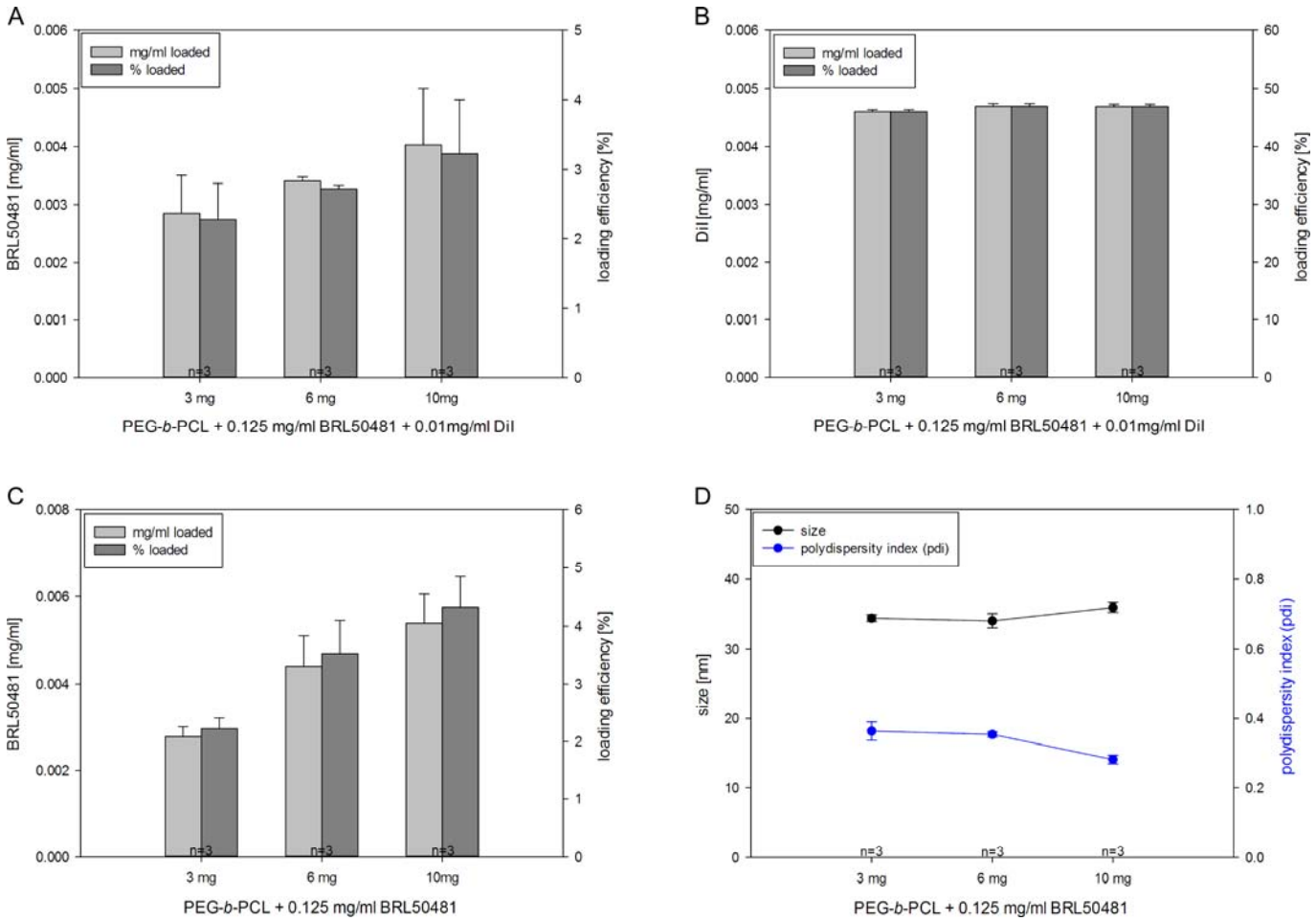


**Figure 17:** Drug (**A, C**) and DiI (**B**) loading content and efficiency of BRL50481 (0.125 mg/ml). Double loading with BRL50481 and DiI did not significantly change the amount of molecules incorporated. **D:** Drug laden NP size did not change when higher amounts of polymer were used.

The total amount of drug incorporated differed not much when drug concentrations above 0.05 mg/ml were used (0.021 – 0.029 mg/ml), however the loading efficiency decreased accordingly (**Fig. 16A**). Additionally there was no effect of drug concentration on NP size (29-35 nm, **Fig. 16B**). Some variations could be observed for the pdi (0.15-0.65), however no clear trend was noticeable (**Fig. 16B**). Therefore further investigations were performed with lower drug amounts (0.125 mg/ml). The amount of BRL50481 could be increased, when higher concentrations of polymer were used (from 0.0028 to 0.0054 mg/ml, **Fig. 17A, C**). No change of drug loading was observed comparing NP with or without DiI (**Fig. 17A, C**). Similar DiI loading efficiency was comparable to non-drug-laden NP (**Fig. 17B**; **Fig. 3B**). As observed before for empty NP (**Fig. 2B**) no change in drug-laden NP size was observed when polymer concentrations were changed (**Fig. 17D**).

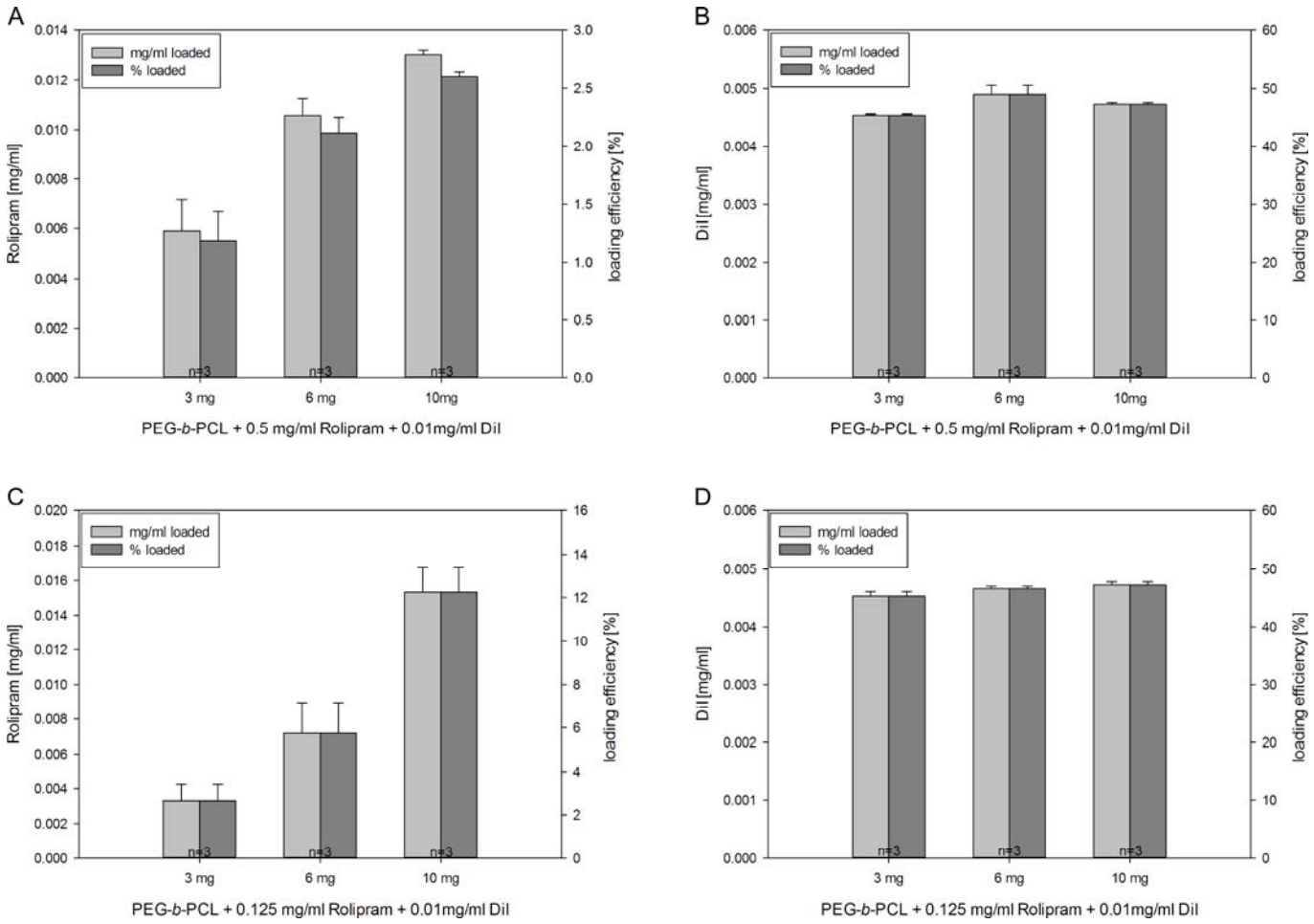


**Figure 18:** Drug (**A, C**) and DiI (**B, D**) loading content and efficiency of Rolipram at different concentrations of polymer with 0.5 (**A, B**) and 0.125 mg/ml Rolipram (**C, D**).

Similar to BRL50481, only low amounts of Rolipram were incorporated by the NP (**Fig. 18A, C**). However the amount could be increased when higher concentrations of polymer were used (from 0.0033 to 0.0153 mg/ml, **Fig. 18A, C**). Lower concentrations of Rolipram (0.125 mg/ml) resulted in similar amounts incorporated into the NP, but increased the loading efficiency (12.25 compared to 2.6%, **Fig. 18A, C**). No change of DiI loading was observed without any (**Fig. 3B**) or different amounts of Rolipram were used (**Fig. 18B, D**).

**8.b. (Month 10-18)** *Identify the drug loading concentration that provides slow release kinetics and sustained delivery for 4 weeks in vitro*

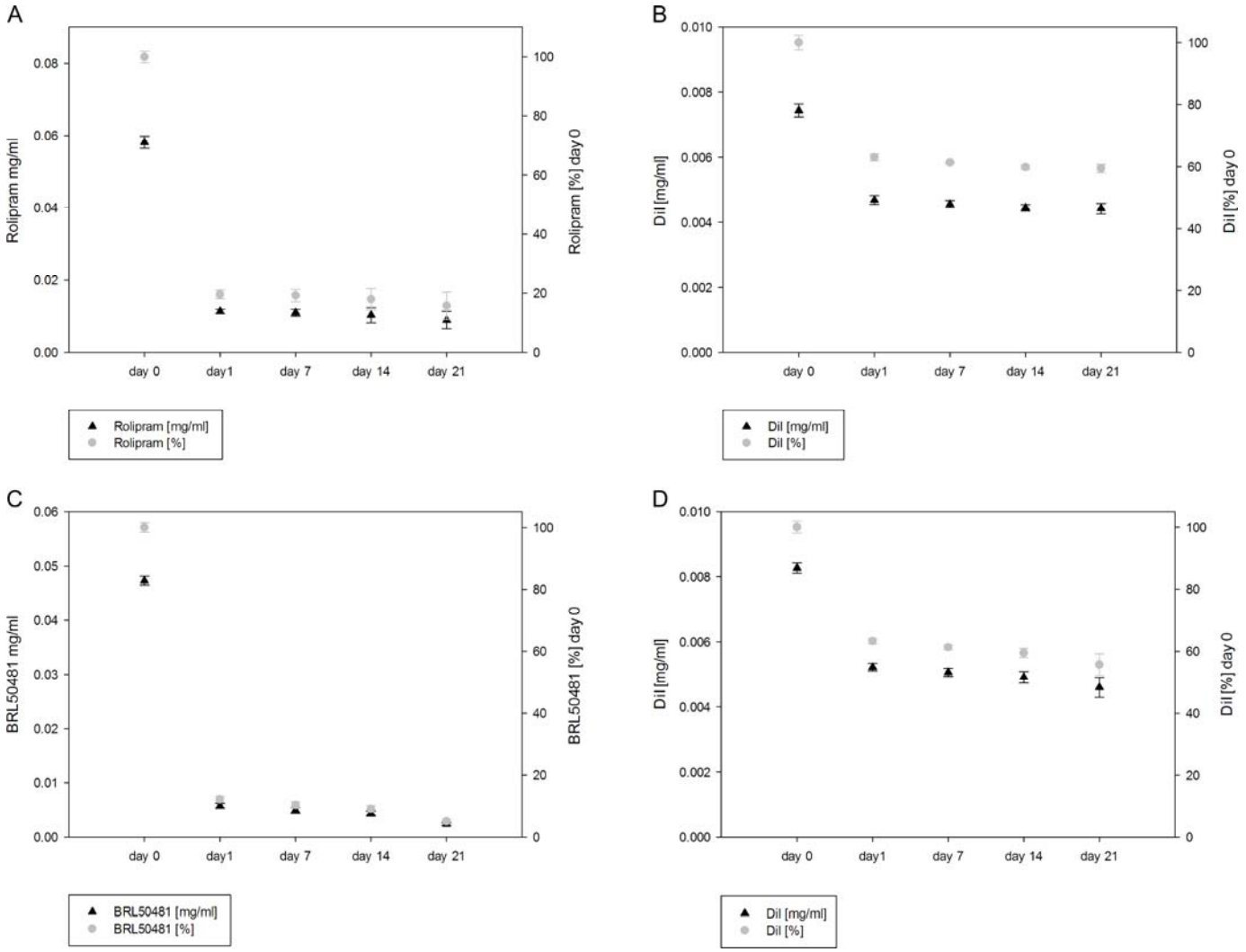


**Figure 19:** Drug release at 37°C. After an initial burst release, Rolipram (**A, B**) and BRL50481 (**C, D**) were slowly released over 3 weeks.

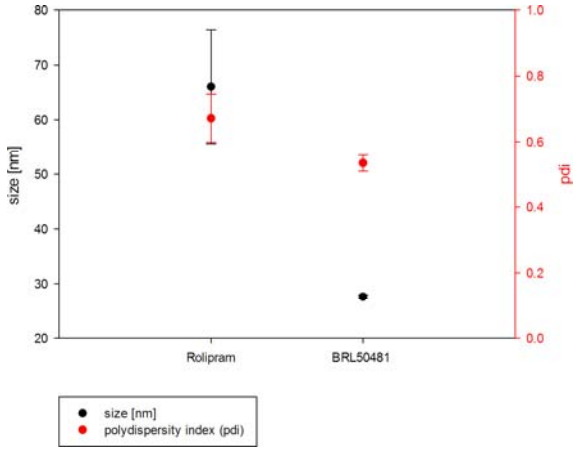


**Figure 20:** NP size of Rolipram- and BRL50481-laden NP, after four weeks at 37°C.

Both PDE-inhibitors as well as DiI were slowly released over a time period of three weeks, after an initial burst release (**Fig. 19**). The burst release is probably due to surface bound molecules. DiI release was similar regardless which drug was incorporated additionally (**Fig. 19B, D**), whereas BRL50481 was released slightly faster than Rolipram (**Fig. 19A, C**). After four weeks nanoparticle

started to aggregate, demonstrated by measuring NP size and pdi (**Fig. 20**). Since absorbance spectra depend on NP size and the aggregation of the particle lead to a shift of the absorbance spectra in a similar fashion, analysis at later time points unfeasible (Pesika et al., 2003). The reasons for the difference in drug (Rolipram, BRL50481) and dye (DiI, DiO) uptake and release between Rolipram and BRL50481 are not defined yet.

**8.c. (Month 10-18)** *Determine the protein adsorption on the NPs by incubation with fluorescent proteins.*

See Task 2c.

**8.d. (Month 13-18)** *Organize obtained chemistry data and discuss final formulations before proceeding*

Polymer concentration of 3 mg and DMF concentration of 28.57% were determined as the optimal formulation to investigate non-functionalized NP in vitro. Inclusion of 10% and 25% aminated PEG-b-PCL+peptide demonstrated the best results regarding fibrin targeting *in vitro*. Due to the lower pdi, 25% aminated PEG-b-PCL+peptide was chosen for further studies. Similar results were obtained for the other peptides (nidogen-1 and versican - DPEAAE, NIDPNAV), which bound to sections of the injured spinal cord. To increase the nanoparticle concentration in solution and accompanying to increase the amount of drug available at the lesion site, the amount of polymer was increased to 6 mg for *in vivo* delivery.

**8.e. (Month 13-24)** *Prepare significant quantities of the different types of drug laden tNPs for in vivo testing [Note: tasks 8a-c will be repeated for each drug with sequential stock production to allow for in vivo testing to take place]*

Different types of NP were shipped to Miami for in vivo testing.

1. Control NP with DiI (0.1 mg/ml, 0.01 mg/ml)
2. Control NP with DiO (0.1 mg/ml, 0.01 mg/ml
3. Control NP with Rolipram (0.125mg/ml)
4. Fibrinogen (10%, 25%, DiI)
5. Fibrinogen (10%, 25%, DiO)
6. Scrambled Fibrinogen (10%, 25%, DiI)
7. Scrambled Fibrinogen (10%, 25%, DiO)
8. Fibrinogen with Rolipram (25%, 0.125 mg/ml, DiI)
9. Scrambled (scr) Fibrinogen with Rolipram (25%, 0.125 mg/ml, DiI)
10. Nidogen-1 (10%, 25%, DiI)
11. Scrambled Nidogen-1 (10%, 25%, DiI)
12. Nidogen-1 with Rolipram (25%, 0.125 mg/ml, DiI)
13. Scrambled Nidogen-1 with Rolipram (25%, 0.125 mg/ml, DiI)
14. Versican (25%)
15. Scrambled Versican (25%)
16. Versican with Rolipram (25%, 0.125 mg/ml)
17. Scrambled Versican with Rolipram (25%, 0.125 mg/ml)

**Milestone 3:** Prepared drug laden tNPs for in vivo efficacy testing after EAE

The drug laden tNPs were made, characterized and shipped for in vivo evaluation following EAE. Milestone 3 was accomplished in Year 2.

**<u>Study Objective 4: Screen drug laden tNPs for in vivo tissue release kinetics as well as anatomical and functional efficacy after EAE [Pearse]</u>**

**Task 9 (Month 13-18):** *Test drug laden tNPs in EAE to optimize tissue delivery and activity*
**9.a.** *Purchase and acclimatize animals*

**9.b.** *Induce EAE in the animals and provide drug encapsulated tNPs (or unmodified NP controls) systemically or directly at the time of first protein production/presence (earliest will be 2 h)*
**9.c.** *Perfuse animals and dissect tissues at 24 h, 3 d, 1 or 3 wk post-infusion*
**9.d.** *Quantify PDE inhibitor drug levels (HPLC), PDE activity (RIA) and/or interferon-1a (immunoblot) levels at the site of the demyelination lesion*
**9.e.** *Identify those tNPs that did not deliver therapeutic levels of the drugs to the site of CNS demyelination for the 3 wk period and re-formulate in vitro (e.g. increase drug load) for re-testing in vivo*
**9.f.** *Re-test any reformulated tNPs*

Animals were ordered to evaluate the spinal cord penetration of drug and target enzyme effects after EAE when the different drug-laden tNPs were intravenously infused versus appropriate unloaded and scrambled peptide controls. In these studies, animals received tNPs beginning at 5 d post-EAE induction i.v. Animals were then evaluated behaviorally using a 0-6 point locomotor deficit score according to the following criteria - 0: no disease; 0.5: distal limp tail; 1: limp tail; 2: mild paraparesis, ataxia; 3: moderate paraparesis, the rats trips from time to time; 3.5: one hind limb is paralyzed, the other moves; 4: complete hind limb paralysis; 5: complete hind limb paralysis and incontinence; 6: moribund, difficulty breathing, does not eat or drink, euthanize immediately. At study endpoint animals were perfused or dissected to allow the examination of histopathology (See Task 10). Analysis of behavioral outcomes (severity of locomotor deficits and initial time of disease onset) showed that all in all Rolipram-laden tNP groups there was a significant reduction in the degree of locomotor deficits as well as the time of initial disease onset was lengthened (**Fig. 21**); the fibrin tNPs showed the most pronounced effects. DiI-laden fibrin tNPs had shown the greatest amount of spinal cord penetration in earlier work (**Fig. 14**).

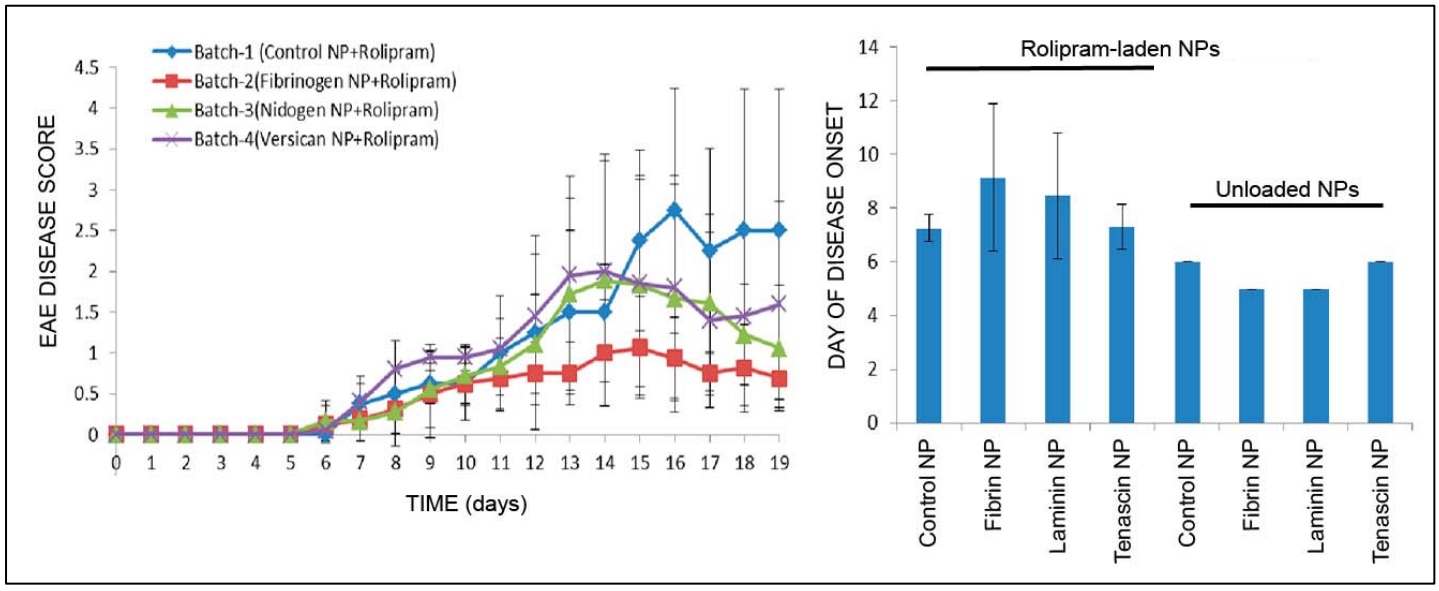


**Figure 21:** Animals receiving infusions of Rolipram-laden tNPs had a reduced severity of disease after EAE induction compared to control, Rolipram-laden NPs (blue line). Only the fibrin tNPs showed a persistent, significant ($p<0.05$) reduction that was present at endpoint, 19 days post-EAE induction, compared to the control (red line). Similarly the day of first disease onset was delayed in those animals receiving tNPs with Rolipram compared to unloaded, control NPs.

**Task 10 (Month 16-24):** *Test the efficacy (anatomical and functional) provided by tNPs (PDE inhibitors, interferon-1a) vs. naked drugs or NP controls after EAE*
**10.a.** *Acclimatize, train and perform baseline functional testing for sensorimotor (catwalk, gridwalk) function*
**10.b.** *Induce EAE in the animals and provide drug encapsulated tNPs (or controls) systemically*

**10.c.** *Perform post-injury behavior analyses on the animals for up to 8 weeks*
**10.d.** *Obtain behavioral data and perform statistical analysis to look for significant differences between treated and untreated control groups*
**10.e.** *Perfuse animals and dissect tissues*
**10.f.** *Obtain fixed tissue, section tissue and examine inflammation, axon demyelination/injury and remyelination repair using immunostaining for specific markers or electronmicroscopy*
**10.g.** *Compare statistically the results between treated and controls*
**10.h.** *Put together a report summarizing the major findings of the behavioral and histological studies with graphs etc.*

Tissue specimens encompassing the L5 spinal cord were embedded and sectioned for histological evaluation. Sections at 200 μm intervals were dye or immunohistochemically stained as following with: (**1**) hematoxylin, eosin and luxol fast blue to quantify the number of perivascular lesions, the area of spinal tissue containing perivascular lesions as well the degree of demyelination, (**2**) immune cell markers CD4, CD8, CD19 and ED1 to examine differences in the tissue infiltration of T cells, B cells and mononuclear phagocytes, respectively, and, (**3**) glial fibrillary acidic protein (GFAP) to investigate the degree of astrogliosis within tissue specimens of control and tNP-treated animals.

We found that, both the size of perivascular lesions as well as the extent of demyelination was significantly reduced in animals receiving Rolipram-laden tNPs (**Fig. 22**), although the number of lesions was unchanged between groups. Animals receiving Rolipram-laden fibrin tNPs showed the most significant reductions in tissue injury. Evaluation of immune cell infiltrates revealed reductions in $CD4^+$ (**Fig. 23**) and $ED1^+$ (**Fig. 24**) cells within the lumbar spinal cord of animals receiving Rolipram-laden tNPs, however, no significant differences in $CD8^+$ and $CD19^+$ cells were obtained (**Table 1**).

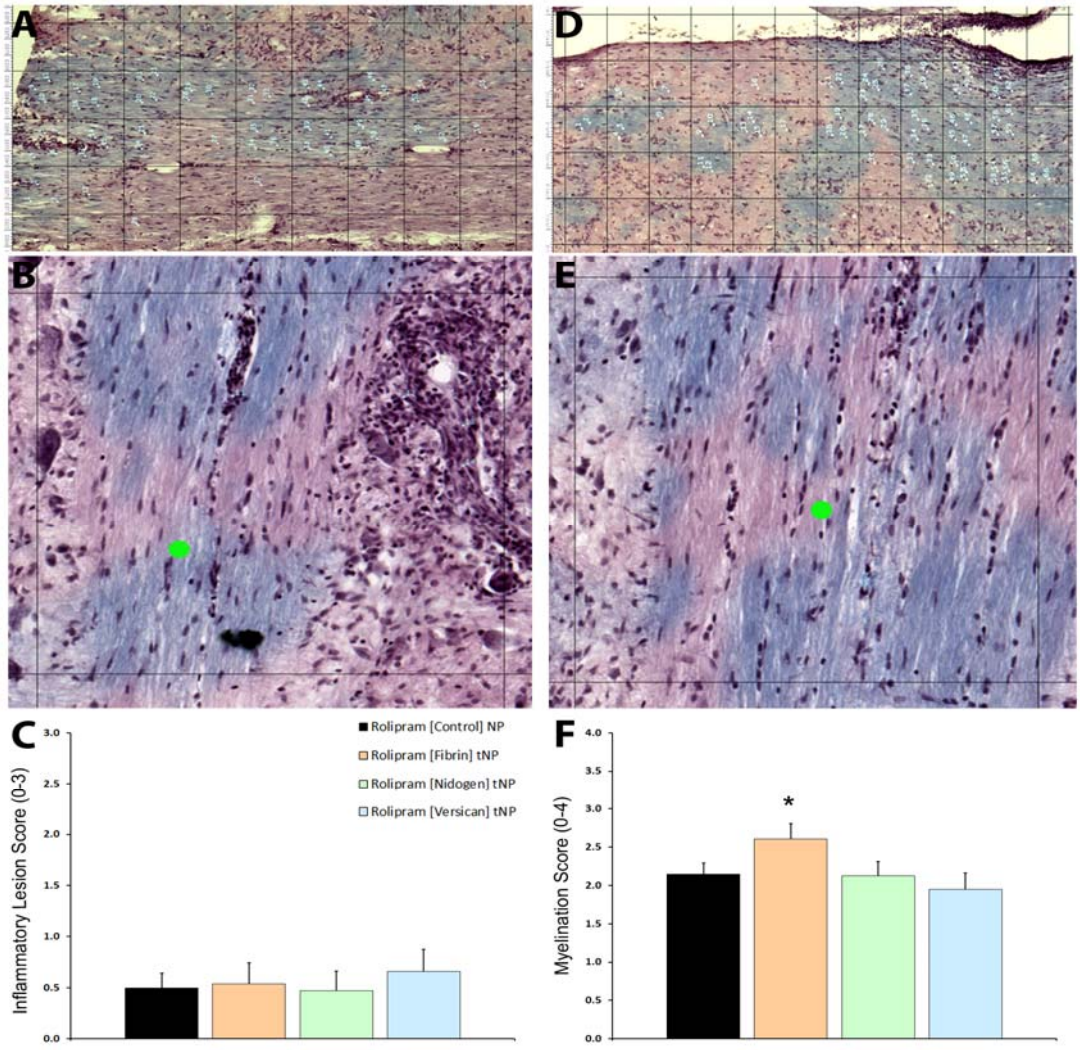

**Figure 22.** Rolipram-laden tNPs do not reduce the number of perivascular lesions, though [Fibrin] tNPs did lessen the degree of demyelination after experimental RRMS. **A-B.** The spinal cord was imaged and divided into grids (**A**) for the counting of perivascular lesions (**B**) and provision of a score from 0-3 (**C**); 0, no perivascular lesions to 3, numerous perivascular lesions. **D-E.** The spinal cord is also divided into grids (**D**) for the quantifying demyelinated regions (**E**) and given a score from 0-4 (**F**); 0, complete demyelination to 4, complete myelination. Statistical significance indicated at *p<0.05.

| *Cell Type* | TREATMENT GROUP | | | |
|---|---|---|---|---|
| | *Rolipram NPs (Control)* | *Rolipram tNPs (Fibrin)* | *Rolipram tNPs (Nidogen)* | *Rolipram tNPs (Versican)* |
| $ED1^+$ | +++ | + | +++ | ++++ |
| $CD4^+$ | ++++ | +++ | ++++ | ++++ |
| $CD8^+$ | ND | ND | ND | ND |
| $CD19^+$ | ND | ND | ND | ND |
| $GFAP^+$ | Pronounced reactivity | Pronounced reactivity | Limited reactivity | Limited reactivity |
| +', Few cells; '++', Mild cell infiltrates; '+++', Moderate cell infiltrates; '++++', Severe cell infiltrates; 'ND', no diff. between groups | | | | |

**Table 1.** Qualitative evaluation of cellular infiltration and reactivity following RRMS among groups. Reductions in $ED1^+$ and $CD4^+$ cell infiltrates were observed with Rolipram [Fibrin] tNPs compared to controls.

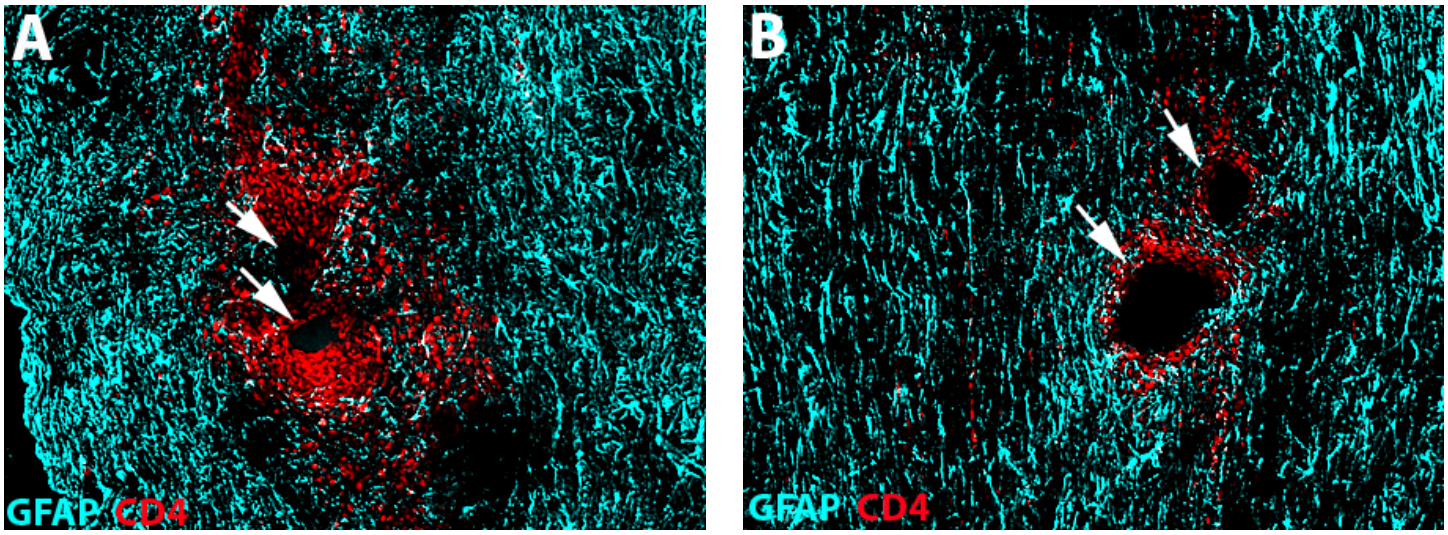


**Figure 23.** $CD4^+$ cell infiltrates at perivascular lesion sites in the lumbar spinal cord. Although numbers of perivascular lesions (indicated by the white arrows) were unchanged between control (**A**) and Rolipram-laden [Fibrin] tNP (**B**) groups, the size of the lesions as well as the number of infiltrating immune cells, in this case $CD4^+$ cells, was significantly reduced in the treatment group (**B**).

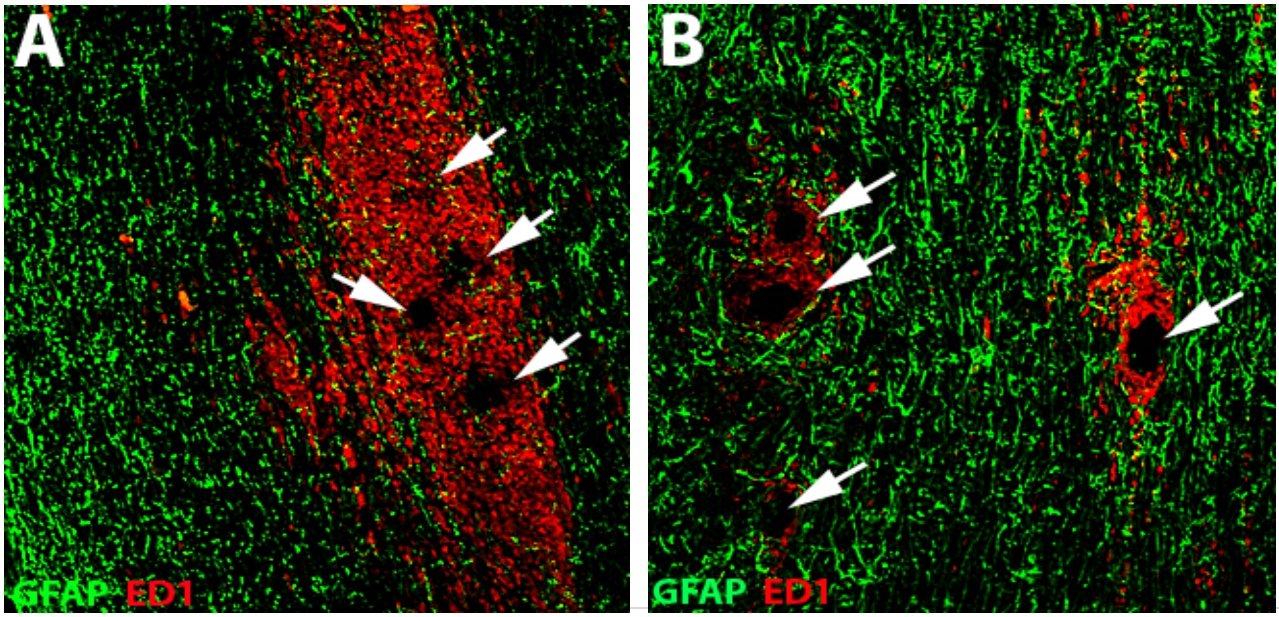

**Figure 24.** ED1$^+$ cell infiltrates at perivascular lesion sites in the lumbar spinal cord. In addition to a reduction in the numbers of infiltrating CD4+ cells, the amount of ED1+ cells (mononuclear phagocytes) was also less at perivascular lesion sites (indicated by the white arrows) in animals receiving Rolipram-laden [Fibrin] tNPs (**B**) compared to controls (**A**).

**Milestone 4:** Identified an effective drug-laden tNP strategy for therapeutic application to RRMS

We have shown that Rolipram-laden tNPs functionalized with peptides recognizing fibrin retard disease progression in this experimental EAE model as measured through specific behavioral and histological outcomes. Milestone 4 was accomplished in Year 2.5.

**Task 11 (Month 22-24):** *Finalize study results*

**11.a.** *Compile all results of the study into a final report*

**11.b.** *Submit any meeting abstracts, manuscripts or patents*

**11.c.** *Prepare a proposal for additional pre-clinical work and the initiation of IND paperwork for requesting a Phase 1 safety study in RRMS patients with the optimal therapeutic approach*

We have completed both *in vitro* and *in vivo* work on the characterization and therapeutic efficacy of drug-laden NPs for targeting disease progression in an experimental model of RRMS. The project data is currently being organized into two manuscripts, the first of which will report on the design, characterization, peptide functionalization and CNS targeting of PEG-PCL NPs *in vitro* and after RRMS (to be submitted to *Nanomedicine*; this manuscript will provide data on all functionalized NPs *in vitro* and *in vivo* and will replace the previous manuscript in preparation; Peptide Functionalized PEG-block-PCL Nanoparticles for Targeting Fibrin Clots, *Journal of Controlled Release*). The second manuscript will present work on the incorporation of hydrophobic drugs (PDE inhibitors) in PEG-PCL NPs, their temporal release kinetics and therapeutic efficacy (behavioral and histological) in an experimental model of RRMS (to be submitted to *The Journal of Neuropathology and Experimental Neurology*). The data will also be used to seek further funding for pre-clinical studies that will drive this technology towards clinical implementation.

**Milestone 4:** Publication of findings

The work performed to date has resulted in two scientific meeting abstracts (See Appendix 1) and will lead to the submission of two manuscripts. Data generated from these investigations will be used to further optimize this technology for pre-clinical evaluation and transition to clinical testing. This pre-clinical work will focus specifically on enhancing the amount of drug that can be incorporated into the tNPs and examining a more prolonged administration paradigm (> 2 days).

Summary of Problems encountered for Project.

- Personnel in Brisbane arrived three months after official starting date of award. Furthermore obtain a necessary introduction to work in the labs additionally delayed the onset of the practical work.
- Long lasting defect in freeze/dryer prevented a more in depth investigation of the long term storage of nanoparticles.
- No peptide sequence to bind to myelin is available momentarily, which makes targeting MBP with our methods impossible at present.
- Additional optimization of flow cytometry procedures was required to ensure avoidance of cell aggregates and the quantification of immune cell populations from lumbar cord homogenates; alternatively, immunohistochemical evaluation of immune cell populations using specific markers was performed.
- Versican tNPs showed limited lumbar spinal cord accumulation – a longer or better-timed administration window or alternative targeting peptide may be required.
- PDE inhibitor drug incorporation into the NPs was lower than expected, 3-12%, compared to up to 80% with fluorescent agents e.g. DiO and DiI.
- We were unable to obtain sufficient incorporation of interferon-1a into PEG-PCL NPs.

## KEY RESEARCH ACCOMPLISHMENTS

- We were able to obtain nanoparticle formation with the poly(ethylene glycol-b-ε-caprolactone) blockpolymer (PEG-b-PCL)
- We were able to develop methodologies that simplified the nanoparticle preparation process
- We were able to incorporate fluorescent dyes into the nanoparticles that could then enable their *in vitro* and *in vivo* tracking
- We demonstrated that aminated (PEG-b-PCL) could be integrated into the development of the (PEG-b-PCL) nanoparticles
- We were able to functionalize the aminated nanoparticles with targeting peptides
- We were able to incorporate the PDE-inhibitors Rolipram and BRL50481 within the nanoparticles
- We provided evidence that, compared to standard PEG-b-PCL nanoparticles, fibrin functionalized nanoparticles possessed greater gel retention with fibrinogen
- We demonstrated that, compared to standard PEG-b-PCL nanoparticles, nidogen-1 and versican functionalized nanoparticles possessed improved binding to sections of injured spinal cord
- We thoroughly characterized of the different types of nanoparticles that were prepared for *in vivo* evaluation (size, pdi, ζ-potential, binding, protein adsorption)
- We characterized the temporal evolution of histopathological and behavioral deficits of an experimental EAE model that mirrors RRMS
- We characterized the temporal expression of important ECM proteins and their natural ligands within the CNS in an experimental RRMS model
- We demonstrated that, compared to a lack of CNS accumulation of NPs that were not functionalized, tNPs (for nidogen-1 and fibrin) can be targeted to CNS lesions after EAE (**feasibility of the technology**)
- We demonstrated that Rolipram-laden tNPs (fibrin) retard disease progression in an experimental EAE paradigm, both behaviorally and histologically (**effectiveness of the technology**), whereas Rolipram-laden NPs that are not functionalized did not show efficacy

## PERSONNEL RECEIVING SALARY FROM THIS AWARD

| | |
|---|---|
| Dr. Damien D. Pearse | Principal Investigator [Miami] |
| Dr. Paul Dalton | Principal Investigator [Brisbane] |
| Dr. Mousumi Ghosh | Associate Scientist [Miami] |
| Dr. Tobias Fuehrmann | Postdoctoral Associate [Brisbane] |
| Dr. Yong Xu | Research Associate [Miami] |
| Ms. Natalia Guggisberg | Research Associate [Miami] |
| Ms. Maria Chiriboga | Research Associate [Miami] |
| Ms. Wai Man Chan | Research Associate [Miami] |
| Ms. Khine Wai | Research Associate [Miami] |

**REPORTABLE OUTCOMES**

In Year 2, work from these investigations was presented at poster sessions/talks at The World Biomaterials Conference and The Zing Neurodegeneration Symposium (See Appendix 1 for full abstracts).

1. Führmann, T., Ghosh, M., Dargaville, T., Pearse, D.D. and Dalton, P.D. (February, 2012) Peptide functionalized nanoparticles for targeted drug delivery. Abstract and oral presentation, 9th World Biomaterial Congress, Chengdu, China.
2. Ghosh, M., Xu, Y., Führmann, T., Dalton, P.D., Pearse, D.D. (December, 2012) Site-Directed Nanotherapeutics to Abrogate Axonal Demyelination and Injury in an Experimental Model of Multiple Sclerosis. Abstract, The Zing Neurodegeneration Symposium, Cancun, Mexico.

**CONCLUSION (summarizes total work to date)**

In these studies we demonstrated that nanoparticles (NPs) could be successfully generated from a poly(ethylene glycol-b-ε-caprolactone) blockpolymer. These NPs ranged in size from 28-36 nm when polymer or solvent concentrations were changed. The optimal NP formation in regard to size distribution was determined as 28.57% DMF and 3 mg polymer concentrations (6 mg were used for in vivo investigations). The manufactured NPs allowed inclusion of fluorescent dyes (DiI, DiO) and aminated PEG-b-PCL. The peptides (i.e. NQEQVSP, DPEAAE and NIDPNAV) could be conjugated to the aminated PEG-b-PCL and integrated into the NPs. Peptide (e.g. NQEQVSP and NIDPNAV and their scrambled controls) functionalized NPs (fNPs) were slightly larger in size then non-functionalized NPs (range of 30-42 nm). To demonstrate substrate targeting *in vitro*, we showed that Fibrin (NQEQVSP) fNP showed a better adherence then non-functionalized NP to fibrin gels, with 10% and 25% functionalization demonstrating the best adherence. Nidogen-1 (NIDPNAV) and Versican (DPEAAE) functionalized nanoparticle (25%) demonstrated better adherence to sections of the injured spinal cord (contusion type injury, explanted 1 week after injury). NPs and fNPs had no surface charge and a low polydispersity index.

Following *in vitro* characterization, fNPs with the peptides NQEQVSP, DPEAAE and NIDPNAV (10% and 25%), were examined in a model of relapsing-remitting MS in the dark agouti rat. In this experimental model we first characterized temporal histopathological changes, behavioral deficits in locomotor function and protein production and localization of target ECM as well as their natural ligands; all of these features were prominent by 10 days post EAE induction. Ensuing experiments investigated the accumulation of non-functionalized as well as tNPs (25%) at lesions within the lumbar spinal cord when administered systemically and repetitively just prior to and during the appearance of these disease features. It was demonstrated that Nidogen-1 fNPs, but not the non-functionalized NPs or the first formulation of Fibrin fNPs, accumulated at the site of CNS lesions. Subsequent studies with a new formulation of Fibrin, but not Versican, fNPs showed good NP accumulation within spinal cord tissues after EAE induction.

Following the development of functionalized NPs, *in vitro* studies examined drug loading of the particles. PEG-b-PCL NPs were able to be loaded with DiI, Rolipram and BRL-50481 as well as a combination of the agents. Drug concentration was low, but could be increased with increasing amount of polymer. Variation of initial drug concentration had no effect on drug incorporation. Unfortunately, sufficient interferon-1a incorporation into the fNPs could not be obtained. The NP released the drug slowly over a time period of up to 4 weeks. Drug release was measured for up to three weeks, at four weeks aggregation of the particles made it difficult to determine the drug content. However even at four week some NP for further release were detectable. When used *in vivo* following EAE, infusion of Rolipram-laden fNPs, particularly those functionalized with binding peptides for Fibrin, reduced the severity of disease as well as delayed disease onset compared to control NPs. Histological evaluation of tissue specimens revealed that Rolipram-laden fNPs reduced the severity, but not number, of perivascular lesions within the lumbar spinal cord at 20 days after RRMS onset. Additionally, the numbers of infiltrating immune cells ($CD4^+$ and $ED1^+$) were also retarded following

Rolipram-laden fNP administration. No efficacy was observed when Rolipram-laden, non-functionalized NPs (control) were used. In conclusion, we have demonstrated the feasibility of this technology through the development of drug-laden, functionalized NPs. We have also showed the effectiveness of Rolipram-laden fNPs in retarding the behavioral and histological hallmarks of RRMS in an experimental paradigm. Future work will examine if higher concentrations of Rolipram can be incorporated into the fNPs for greater therapeutic efficacy in RRMS and experimental, progressive MS models and whether the systemic delivery of Rolipram-laden fNPs is associated with any observable organ toxicity. The completion of this work will allow us to gather the necessary pre-clinical data for translating this novel approach towards clinical evaluation in human MS.

## REFERENCES


1. B. D. Trapp, L. Bö, S. Mörk, A. Chang, *J Neuroimmunol* **98**, 49 (1999).
2. B. D. Trapp, K.-A. Nave, *Annu Rev Neurosci* **31**, 247 (2008).
3. D. D. Pearse et al., *Nat Med* **10**, 610 (2004).
4. S. H. Francis, J. D. Corbin, *Crit Rev Clin Lab Sci* **36**, 275 (1999).
5. J. A. Beavo, *Physiol Rev* **75**, 725 (1995).
6. J. E. Souness, C. Houghton, N. Sardar, M. T. Withnall, *Br J Pharmacol* **121**, 743 (1997).
7. C. M. Atkins et al., *Exp Neurol* **208**, 145 (2007).
8. K. Wallner, C. Li, M. C. Fishbein, P. K. Shah, B. G. Sharifi, *J Am Coll Cardiol* **34**, 871 (1999).
9. E.-J. Kooi et al., *Neuropathol Appl Neurobiol* **35**, 283 (2009).
10. W. Shen-Guo, Q. Bo, *Polymers for Advanced Technologies* **4**, 363 (1993).
11. K. Letchford, R. Liggins, H. Burt, *J Pharm Sci* **97**, 1179 (2008).
12. N. S. Pesika, K. J. Stebe, P. C. Searson, *Journal of Physical Chemistry B* **107**, 10412 (2003).

# APPENDIX 1: SCIENTIFIC ABSTRACTS



## Peptide functionalized nanoparticles for targeted drug delivery

Tobias Füehrmann[a], Mousumi Ghosh[b], Tim Dargaville[a], Damien D. Pearse[b] and Paul D. Dalton*[a]

[a] *IHBI Queensland University of Technology, 60 Musk Ave, Kelvin Grove, QLD 4059, Brisbane, Australia.*
*Fax: 61 7 3138 6030 ; Tel: 61 7 3138 6285 ; E-mail: tobias.fuhrmann@qut.edu.au*
[b] *The Department of Neurological Surgery, The Miami Project to Cure Paralysis, University of Miami Miller School of Medicine, Miami, Florida*

### Introduction

Nanomedicine is becoming prevalent in research and is beginning to move into the clinic [1]. The use of intravenous (i.v.) nanoparticle (NP) delivery is an area of great interest and there is evidence that drug delivery using NP has therapeutic effects on the injured central nervous system. The local administration of methylprednisolone releasing NP to the injured spinal cord results in reduced lesion volume and improved behavioural outcomes, using low levels of the drug [2]. However, the introduction of NP into the bloodstream does not necessarily result in the accumulation of a therapeutic agent at the site of injury. Targeting aims to improve NP aggregation in specific tissue(s). Here we describe peptide functionalized NPs, targeted to bind to the extracellular matrix (ECM) protein nidogen at the lesion site of animals with experimental autoimmune encephalomyelitis (EAE).

### Materials & Methods

Amphilic poly(ethylene glycol-b-ε-caprolactone) (PEG-b-PCL, $M_n x10^3$: 2-b-2.8, $M_w/M_w$: 1.15) nanoparticles (**NP**) were surface-functionalized by inclusion of peptide-conjugated α-amino-ω-hydroxy terminated PEG-b-PCL ($M_n x10^3$: 5.8-b-19, $M_w/M_n$: 1.4) (**tNP**) blockpolymer. Naïve NP and scrambled peptide-conjugated NP were used as controls (**scr. tNP**). Spinal cord homogenates of dark agouti rats (Charles River) in complete Freund's adjuvant were used for EAE induction. Animals were analysed for the target protein by immunohistochemistry and immunoblotting 5, 10 and 15 days post EAE-induction. Nanoparticles (NP, 25% tNP & 25% scr. tNP) were injected i.v. beginning 10 days post EAE-induction for 2 days. After 2 days NP localization within the lumbar spinal cord was examined by confocal microscopy.

### Results & Discussion

The size range of naïve, scrambled peptide control and peptide NPs was 28-38nm. The smallest diameter was observed with the naïve NPs (27.77 nm) whereas the scrambled peptide control (25%) had the largest diameter (38.19 nm). All NPs had practically no surface charge and a low polydispersity index (pdi). For a complete overview see Table 1. Immunoblotting for the ECM protein laminin and its natural ligand nidogen within lumbar spinal cord homogenates from naïve animals and animals with EAE revealed a small increase in production of both proteins within 5 days of EAE-induction over naïve levels. Both proteins demonstrated prominent and significant ($p<0.01$) increases by 15 days post-induction. Immunohistochemistry revealed that these proteins were highly concentrated within regions of blood-brain-barrier (BBB) breakdown, immune cell infiltration and tissue damage. Lumbar spinal cords from EAE animals receiving control, DiI-laden NP failed to show fluorescent NP within tissue sections. In contrast, nidogen DiI-laden tNP (25%) were found localized throughout white matter lesions after i.v. infusion (Fig.1.)

**Fig. 1:** Successful targeting of nidogen within the lumbar spinal cord by nidogen-targeted NP (25%; red dots,).

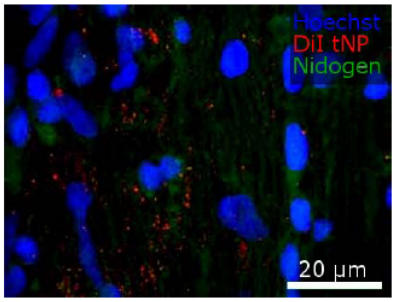


**Table 1**. NP size, charge and polydispersity index (pdi)

| | size | charge | pdi |
|---|---|---|---|
| NP | 27.77±0.38 | 0.07±0.55 | 0.16±0.014 |
| 1% tNP | 28.73±0.68 | -1.28±0.66 | 0.33±0.062 |
| 5% tNP | 29.98±1.34 | 0.48±1.52 | 0.17±0.018 |
| 10% tNP | 29.42±0.77 | 0.85±0.91 | 0.36±0.042 |
| 25% tNP | 33.19±0.45 | -0.85±0.66 | 0.18±0.02 |
| 1% scr. tNP | 27.75±0.65 | -0.45±0.51 | 0.15±0.021 |
| 5% scr. tNP | 27.88±0.49 | -0.26±0.99 | 0.18±0.0196 |
| 10% scr. tNP | 30.14±0.35 | -2.06±0.81 | 0.15±0.008 |
| 25% scr. tNP | 38.19±0.64 | -0.17±0.3 | 0.12±0.015 |

### Conclusion

The data demonstrates that ECM targeting of NPs with peptides is feasible *in vivo*. While the targeting here is aimed at the central nervous system after EAE-induction, it is envisioned that any tissue damage involving ECM up-regulation can be treated with surface modified, drug-laden NP. The actual quantity of the pharmaceutical in the body will be a magnitude lower than the currently employed systemic injection procedure, putatively reducing unwanted side-effects of the agent.

### Acknowledgments

This work was supported by grant #MS090180 from the USAMRAA.

### References

1 Maurer-Jones M.A., Bantz K.C., Love S.A., Marquis B.J., Haynes C.L. *Nanomedicine (Lond)*, 2009, **4**, 219;
2 Kim Y.T., Caldwell J.M., Bellamkonda R.V. *Biomaterials*, 2009, **30**, 2582

# Site-Directed Nanotherapeutics to Abrogate Axonal Demyelination and Injury in an Experimental Model of Multiple Sclerosis

**Mousumi Ghosh[a], Yong Xu[a], Tobias Führmann[b], Paul D. Dalton[b] and Damien D. Pearse[a*]**

[a] *The Department of Neurological Surgery, The Miami Project to Cure Paralysis, University of Miami Miller School of Medicine, Miami, Florida, USA.*
[b] *IHBI Queensland University of Technology, 60 Musk Ave, Kelvin Grove, QLD 4059, Brisbane, Australia.*

Multiple sclerosis (MS) is an inflammatory demyelinating disease of the human central nervous system (CNS). Phosphodiesterase (PDE)-4 inhibitors, which prevent the hydrolysis of cyclic AMP, has been demonstrated to reduce inflammation, prevent tissue damage and provide functional benefit in the experimental autoimmune encephalomyelitis (EAE) experimental model of MS. In the current study we determined whether Rolipram, a PDE4 inhibitor, when contained within amphilic PEG-PCL nanoparticles (NP) would provide a novel and effective means of reducing disease progression and avoid the drug's known systemic side-effects. Further, these NPs were surface modified with specific peptides that recognize proteins extravasated at sites of vascular disruption (clotting factors, extracellular matrix) to enhance their accumulation and Rolipram delivery to regions of CNS demyelination. In initial work we employed DiI labelled, peptide functionalized NPs (fNP), targeted to bind to the different ECM (nidogen, tenascin-c or fibrinogen) or their scrambled controls. We demonstrate in an experimental model of relapsing-remitting (RR)- EAE in the Dark Agouti rat that in contrast to non-functionalized DiI-NPs, which failed to accumulate at sites of white matter lesions following systemic administration, at an optimal window just prior to appearance of pathological changes and pronounced functional deficits, delivery of functionalized DiI- labelled NPs that are conjugated to specific peptides targeted to these ECM were found to be sequestered to CNS lesions indicating that ECM targeting of NPs with peptides is feasible in vivo. Of the three different functionalized NP's employed, NPs conjugated to both Nidogen and Fibrin showed maximal adherence to the lesion site compared to NPs conjugated with scrambled peptides. Experiments were further performed using functionalized NPs incorporated with Rolipram and administered in vivo following induction of EAE and therapeutic efficacy of the drug incorporated fNP was determined based on assessment of clinical scores and histopathological examination of the lumbar cord region of the test animals compared to control animals that were either injected with fNPs alone or treated with direct administration of Rolipram. Our results indicated both Nidogen and fibrin tNPs, accumulated at the site of CNS lesions indicating to be the optimal peptide for functionalizing NPs, although the most efficacious therapeutic targeting of Rolipram determined based on reduction of clinical symptoms, was obtained only with fibrin fNPs that were conjugated to Factor XIIIa peptide (NQEQVSP) compared to Rolipram contained fNPs targeted towards other ECM such as Nidogen or Tenascin-C or following direct systemic administration of Rolipram.. Histopathological analysis of the CNS is currently ongoing to determine if the reduction in clinical symptoms observed with Rolipram incorporated fibrin targetted NPs correlates to abrogation of axonal demyelination /reduced lesion formation.

Acknowledgments: This work was supported by grant #MS090180 from the USAMRAA.